MDS.[13–15] In fact, the prognostic value of these two chromosome aberration groups was not significantly different among AML patients,[15] but sufficient data for MDS were lacking. The present study demonstrates that the prognosis of patients who carry −5 and del(5q) are significantly different, as OS and LFS of −5 group were shorter than del(5q) patients even if 5q- syndrome patients were excluded from del(5q) patients (Figure 2 and data not shown). AML patients with monosomy 7 rather than with deleted 7q chromosome were reported to lead to poor prognosis.[16] Significantly poor prognosis of −5 group in our series might be explained by the observation that −5 was significantly correlated with presence of monosomy 7 as compared to del(5q) group ($P<0.001$). The co-presence of chromosomes 5 and 7 abnormalities has been associated with poor outcomes in MDS and AML.[17–22]

Although the cause of leukemic progression is unknown, susceptibility to leukemia clearly leads to higher mortality of −5 patients compared to del(5q) patients (Figure 2b). The −5 group also had significantly more severe neutropenia and thrombocytopenia and might exacerbate the survival of this group (Figures 1b and c). Neutropenia and thrombocytopenia, but not severe anemia, are reported to be common findings of patients with monosomy 7.[23] Taken together, laboratory findings shown in −5 group and high incidence of the co-presence of −5 and monosomy 7 might result in poor prognosis of the corresponding patients.

In this survey, the incidence of 5q- syndrome was quite rare in Japan. Recent studies suggest different genetic or environmental backgrounds between Asian and Western MDS populations.[24,25] According to the recent report by Haase *et al.*,[28] isolated del(5q) was seen in 14%, del(5q) with one additional abnormality in 5%, and complex abnormalities including del(5q) were seen in 11% of patients with clonal abnormalities. In the Korean study, isolated del(5q) was seen in 1.7% of the patients.[24] The incidence of del(5q), isolated del(5q) and 5q- syndrome patients was 8.4, 2.2 and 1.3%, respectively, in Japanese MDS study. These data are lower than those of Western patients but more similar to those of Asian patients.[24–26]

In the present study, we paid particular attention to MDS patients with del(5q) and classified them into four groups according to the cytogenetic complexity: 5q-, 7+, complex and other. 5q- patients have previously been well defined as having relatively good prognosis, whereas poor prognosis was indicated when it was combined with other anomalies.[19,20,26,27] OS and LFS of 7+ group were significantly shorter than 5q- group and OS of complex was significantly shorter than 5q-(Figure 3a and data not shown). It is suggested that the clinical outcome of MDS patients with del(5q) depends on the prognostic value of combined chromosomal abnormalities.

The most significant independent prognostic variables in MDS are the percentage of bone marrow blasts, the number of cytopenias and cytogenetic pattern. By weighting these variables according to their statistic power, IPSS separates MDS patients into four distinct risk groups regarding survival and the potential for leukemic progression: low risk, Int-1, Int-2 and high risk.[10] Even in the del(5q) patient group, which is considered to have a better prognosis, univariate analysis and multivariate analysis of del(5q) patients in our series showed that the cytogenetic pattern, percentage of bone marrow blasts and platelet transfusion dependency were the most relevant risk factors (Tables 2 and 3). Figures 3b and c show that IPSS critically determines OS and LFS of del(5q) patients. All 21 patients classified as 5q- syndrome were low risk of IPSS, and the patients classified as high risk were AML and refractory anemia with excess blasts (RAEB)-2 cases with adverse chromosomal abnormalities.

As for the del(5q) patients who are far from the risk of leukemic progression, red cell transfusion dependency often has an adverse impact on survival.[28] Although red cell transfusion dependency was not a significant prognostic factor by the present analyses, the degree of anemia had a tendency to affect survival of these patients from the result of univariate analysis ($P=0.059$, Table 2).

Although IPSS is based on FAB classification and does not take into account other prognostic factors such as dysplasia and transfusion requirement, WPSS has a relevant prognostic value.[29] Therefore, we applied WPSS to our patient data (Figure 3d) and confirmed that WPSS can predict the prognosis of del(5q) MDS patients more clearly than IPSS.

Our study demonstrated that −5 and del(5q) belong to different clinical entities and their biological behaviors are different from each other, and that del(5q) patients can be stratified according to their additional chromosomal abnormalities and IPSS or WPSS status. Severe anemia requires frequent transfusions, reduces quality of life and becomes often the major clinical problem for MDS patients with del(5q). The prognosis of del(5q) patients is related to their status of chromosomal abnormalities and transfusion dependency, but new agents such as lenalidomide improve the disorder and might provide new insights into more precise understanding of the disease.[30]

Acknowledgements

We greatly thank the hospitals that provided patient data as described in the Supplementary Information, and also thank Ms Aki Tochigi for the paper preparation. This study was supported by the grant of the Japanese Cooperative Study Group for Intractable Bone Marrow Diseases, Ministry of Health, Labor and Welfare of Japan.

References

1 Nimer SD, Golde DW. The 5q- abnormality. *Blood* 1987; **70**: 1705–1712.
2 Van den Berghe H, Michaux L. 5q-, twenty-five years later: a synopsis. *Cancer Genet Cytogenet* **94**: 1–7.
3 Giagounidis AA, Germing U, Haase S, Hildebrandt B, Schlegelberger B, Schoch C *et al.* Clinical, morphological, cytogenetic, and prognostic features of patients with myelodysplastic syndromes and del(5q) including band q31. *Leukemia* 2004; **18**: 113–119.
4 Giagounidis AA, Germing U, Wainscoat JS, Boultwood J, Aul C. The 5q- syndrome. *Hematology* 2004; **9**: 271–277.
5 Van den Berghe H, Cassiman JJ, David G, Fryns JP, Michaux JL, Sokal G. Distinct haematological disorder with deletion of long arm of no. 5 chromosome. *Nature* 1974; **251**: 437–438.
6 Giagounidis AA, Germing U, Strupp C, Hildebrandt B, Heinsch M, Aul C. Prognosis of patients with del(5q) MDS and complex karyotype and the possible role of lenalidomide in this patient subgroup. *Ann Hematol* 2005; **84**: 569–571.
7 Malcovati L, Porta MG, Pascutto C, Invernizzi R, Boni M, Travaglino E *et al.* Prognostic factors and life expectancy in myelodysplastic syndromes classified according to WHO criteria: a basis for clinical decision making. *J Clin Oncol* 2005; **23**: 7594–7603.
8 Van den Berghe H, Vermaelen K, Mecucci C, Barbieri D, Tricot G. The 5q- anomaly. *Cancer Genet Cytogenet* 1985; **17**: 189–255.
9 Greenberg P, Cox C, LeBeau MM, Fenaux P, Morel P, Sanz G *et al.* International scoring system for evaluating prognosis in myelodysplastic syndromes. *Blood* 1997; **89**: 2079–2088.
10 Harris NL, Jaffe ES, Diebold J, Flandrin G, Muller-Hermelink HK, Vardiman J *et al.* World Health Organization classification of neoplastic diseases of the hematopoietic and lymphoid tissues:

report of the Clinical Advisory Committee meeting-Airlie House, Virginia, November 1997. *J Clin Oncol* 1999; **17**: 3835–3849.
11 Malcovati L, Germing U, Kuendgen A, Porta D, Pascutto C, Invernizzi R *et al*. Time-dependent prognostic scoring system for predicting survival and leukemic evolution in myelodysplastic syndromes. *J Clin Oncol* 2007; **25**: 3503–3510.
12 Bennett JM, Catovsky D, Daniel MT, Flandrin G, Galton DA, Gralnick HR *et al*. Proposals for the classification of the myelodysplastic syndromes. *Br J Haematol* 1982; **51**: 189–199.
13 Dastugue N, Payen C, Lafage-Pochitaloff M, Bernard P, Leroux D, Huguet-Rigal F *et al*. Prognostic significance of karyotype in *de novo* adult acute myeloid leukemia. The BGMT group. *Leukemia* 1995; **9**: 1491–1498.
14 Mauritzson N, Johansson B, Albin M, Rylander L, Billstrom R, Ahlgren T *et al*. Survival time in a population-based consecutive series of adult acute myeloid leukemia—the prognostic impact of karyotype during the time period 1976–1993. *Leukemia* 2000; **14**: 1039–1043.
15 Grimwade D, Walker H, Oliver F, Wheatley K, Harrison C, Harrison G *et al*. The importance of diagnostic cytogenetics on outcome in AML: analysis of 1612 patients entered into the MRC AML 10 trial. The Medical Research Council Adult and Children's Leukaemia Working Parties. *Blood* 1998; **92**: 2322–2333.
16 Hasle H, Alonzo TA, Auvrignon A, Behar C, Chang M, Creutzig U *et al*. Monosomy 7 and deletion 7q in children and adolescents with acute myeloid leukemia: an international retrospective study. *Blood* 2007; **109**: 4641–4647.
17 Morel P, Hebbar M, Lai JL, Duhamel A, Preudhomme C, Wattel E *et al*. Cytogenetic analysis has strong independent prognostic value in *de novo* myelodysplastic syndromes and can be incorporated in a new scoring system: a report on 408 cases. *Leukemia* 1993; **7**: 1315–1323.
18 Toyama K, Ohyashiki K, Yoshida Y, Abe T, Asano S, Hirai H *et al*. Clinical implications of chromosomal abnormalities in 401 patients with myelodysplastic syndromes: a multicentric study in Japan. *Leukemia* 1993; **7**: 499–508.
19 Jacobs RA, Cornbleet M, Vardiman J, Larson R, LeBeau MM, Rowley JD. Prognostic implications of morphology and karyotype in primary myelodysplastic syndromes. *Blood* 1986; **67**: 1765–1772.
20 Yunis JJ, Lobell M, Arnesen MA, Oken MM, Mayer MG, Rydell RE *et al*. Refined chromosome study helps define prognostic subgroups in most patients with primary myelodysplastic syndrome and acute myelogenous leukaemia. *Br J Haematol* 1988; **68**: 189–194.
21 Pierre R, Catovsky D, Mufti G, Swansbury G, Mecucci C, Dewald GW *et al*. Clinical cytogenetic correlations in myelodysplasia (preleukemia). *Cancer Genet Cytogenet* 1989; **40**: 149–161.
22 Samuels BL, Larson RL, LeBeau MM, Daly KM, Bitter MA, Vardiman JW *et al*. Specific chromosomal abnormalities in acute nonlymphocytic leukemia correlate with drug susceptibility *in vivo*. *Leukemia* 1988; **2**: 79–83.
23 Kardos G, Baumann I, Passmore SJ, Locatelli F, Hasle H, Schultz KR *et al*. Refractory anemia in childhood: a retrospective analysis of 67 patients with particular reference to monosomy 7. *Blood* 2003; **102**: 1997–2003.
24 Lee JH, Lee JH, Shin YR, Lee JS, Kim WK, Chi HS *et al*. Application of different prognostic scoring systems and comparison of the FAB and WHO classifications in Korean patients with myelodysplastic syndrome. *Leukemia* 2003; **17**: 305–313.
25 Chen B, Zhao WL, Jin J, Xue YQ, Cheng X, Chen XT *et al*. Clinical and cytogenetic features of 508 Chinese patients with myelodysplastic syndrome and comparison with those in Western countries. *Leukemia* 2005; **19**: 767–775.
26 Sokal G, Michaux JL, van den Berghe H, Cordier A, Rodhain J, Ferrantr A *et al*. A new hematologic syndrome with a distinct karyotype: the 5q- chromosome. *Blood* 1975; **46**: 519–533.
27 Dewald GW, Davis MP, Pierre RV, O'Fallon JR, Hoagland HC. Clinical characteristics and prognosis of 50 patients with a myeloproliferative syndrome and deletion of part of the long arm of chromosome 5. *Blood* 1985; **66**: 189–197.
28 Haase D, Germing U, Schanz J, Pfeilstöcker M, Nösslinger T, Hildebrandt B *et al*. New insights into the prognostic impact of the karyotype in MDS and correlation with subtypes: evidence from a core dataset of 2124 patients. *Blood* 2007; **110**: 4385–4395.
29 Malcovati L, Porta MG, Pascutto C, Invernizzi R, Boni M, Travaglino E *et al*. Prognostic factors and life expectancy in myelodysplastic syndromes classified according to WHO criteria: a basis for clinical decision making. *J Clin Oncol* 2005; **23**: 7594–7603.
30 List AF, Baker AF, Green S, Bellamy W. Lenalidomide: targeted anemia therapy for myelodysplastic syndromes. *Cancer Control* 2006; **13**: 4–11.

Supplementary Information accompanies the paper on the Leukemia website (http://www.nature.com/leu)

Cell Stem Cell
Article

Evi-1 Is a Critical Regulator for Hematopoietic Stem Cells and Transformed Leukemic Cells

Susumu Goyama,[1] Go Yamamoto,[1] Munetake Shimabe,[1] Tomohiko Sato,[1] Motoshi Ichikawa,[1] Seishi Ogawa,[1,2,3] Shigeru Chiba,[1,2] and Mineo Kurokawa[1,*]
[1]Department of Hematology and Oncology
[2]Department of Cell Therapy and Transplantation Medicine
[3]Department of Regeneration Medicine for Hematopoiesis
Graduate School of Medicine, University of Tokyo, The University of Tokyo Hospital, 7-3-1 Hongo, Bunkyo-ku, Tokyo 113-8655, Japan
*Correspondence: kurokawa-tky@umin.ac.jp
DOI 10.1016/j.stem.2008.06.002

SUMMARY

Evi-1 has been recognized as one of the dominant oncogenes associated with murine and human myeloid leukemia. Here, we show that hematopoietic stem cells (HSCs) in *Evi-1*-deficient embryos are severely reduced in number with defective proliferative and repopulating capacity. Selective ablation of Evi-1 in Tie2$^+$ cells mimics Evi-1 deficiency, suggesting that Evi-1 function is required in Tie2$^+$ hematopoietic stem/progenitors. Conditional deletion of Evi-1 in the adult hematopoietic system revealed that *Evi-1*-deficient bone marrow HSCs cannot maintain hematopoiesis and lose their repopulating ability. In contrast, Evi-1 is dispensable for blood cell lineage commitment. *Evi-1*$^{+/-}$ mice exhibit the intermediate phenotype for HSC activity, suggesting a gene dosage requirement for Evi-1. We further demonstrate that disruption of Evi-1 in transformed leukemic cells leads to significant loss of their proliferative activity both in vitro and in vivo. Thus, Evi-1 is a common and critical regulator essential for proliferation of embryonic/adult HSCs and transformed leukemic cells.

INTRODUCTION

The ecotropic viral integration site-1 (*Evi-1*) gene was first identified as a common locus of retroviral integration in myeloid tumors in AKXD mice (Mucenski et al., 1988). In humans, *Evi-1* is located on chromosome 3q26, and rearrangements on chromosome 3q26 often activate *Evi-1* expression in acute myeloid leukemia (AML) and myelodysplastic syndrome (MDS) (Ogawa et al., 1996; Suzukawa et al., 1994). Although these rearrangements are infrequent in AML, they are of remarkable prognostic value. Patients with these karyotypes are characterized by the elevated platelet count and lack of response to antileukemic therapy (Pintado et al., 1985). Elevated *Evi-1* expression occurs with high frequency in AML patients without 3q26 abnormalities and is also associated with unfavorable outcomes (Barjesteh van Waalwijk van Doorn-Khosrovani et al., 2003; Valk et al., 2004). Thus, Evi-1 is one of the key factors that predict poor survival in leukemia patients.

Evi-1 is a member of the SET/PR domain family of transcription factors, and it contains a total of ten zinc finger motifs organized in two discrete domains, located at the N terminus and toward the C terminus, comprising seven (ZF1) and three (ZF2) repeats, respectively, which have distinct DNA-binding specificities (Delwel et al., 1993; Perkins et al., 1991). The alternative forms generated from the *Evi-1* gene include at least three distinct proteins: Evi-1a, Evi-1b, and Evi-1c (MDS1-Evi-1) (Fears et al., 1996; Hirai, 1999; Figure 1A). Structurally in Evi-1c, a conserved PR domain is located at the N terminus of the Evi-1a. Thus, PR-containing (Evi-1c) and PR-absent (Evi-1a) forms of Evi-1 exist, both of which are expressed in several developing and adult tissues. Although related, functional differences between Evi-1a and Evi-1c have been documented (Nitta et al., 2005; Sood et al., 1999). Another naturally occurring splice variant, designated Evi-1b, has been described, which lacks 324 internal amino acids, including zinc fingers 6 and 7 of ZF1 (Bordereaux et al., 1990). The biological function of Evi-1b is not known thus far.

Previous studies revealed that Evi-1 possesses diverse functions as an oncoprotein. Evi-1 antagonizes growth-inhibitory effects of transforming growth factor-β (TGF-β) by interacting with Smad3 (Kurokawa et al., 1998); protects cells from stress-induced cell death by inhibiting c-Jun N-terminal kinase (JNK) (Kurokawa et al., 2000); increases the expression of endogenous c-Jun and c-*fos*, resulting in activation of AP-1 (Tanaka et al., 1994); and blocks granulocytic differentiation of myeloid cells (Morishita et al., 1992). In addition, Evi-1 interacts with corepressor CtBP, and this interaction contributes to Evi-1-mediated repression of TGF-β signaling (Izutsu et al., 2001). Furthermore, mouse models for Evi-1 overexpression have been established using bone marrow infection and transplantation. These studies showed that activation of Evi-1 in hematopoietic cells leads to myeloid dysplasia while the development of full-blown leukemia requires additional genetic events (Buonamici et al., 2004; Jin et al., 2007).

The mutant mice with disrupted *Evi-1* have been generated (Hoyt et al., 1997). The homozygous embryos tend to exhibit widespread hypocellularity, hemorrhaging, and disruption in the development of paraxial mesenchyme, resulting in the death in utero at approximately embryonic day 10.5 (E10.5). However, these mice carry a targeted deletion of exon 7, resulting in an isoform-specific null for the longer Evi-1 transcripts (Evi-1a and Evi-1c), whereas the truncated form of Evi-1 (Evi-1b) remains unaltered (Figure 1A). Therefore, the remaining expression of

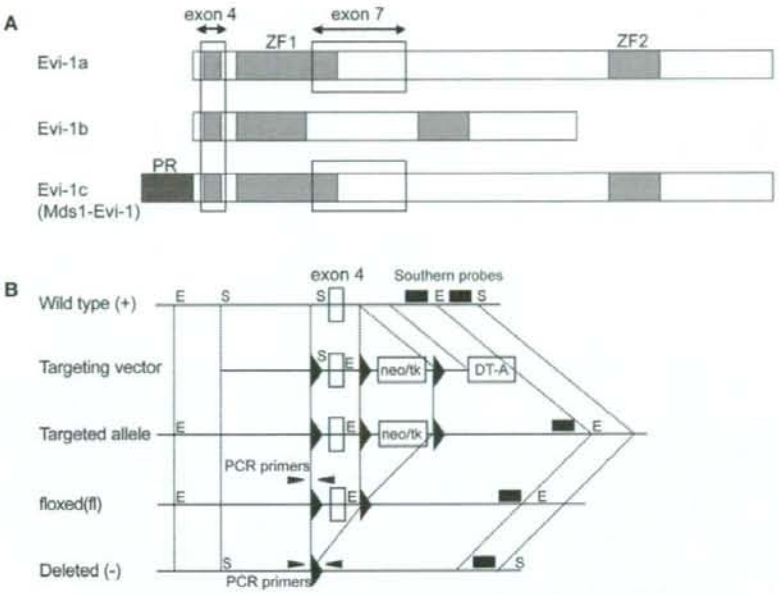

E

	wild	Evi-1(+/-)	Evi-1(-/-)	total
E9.5	2	6	4	12
E10.5	8	9	4	21
E11.5	4	7	4	15
E12.5	5	5	2	12
E13.5	8	12	1	21
E14.5	11	32	5	48
E15.5	5	20	3	28
E16.5	6	12	2	20
E18.5	4	12	1*	17
Pups	14	30	0	44

* Degenerated

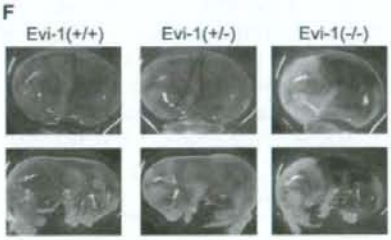

Figure 1. Generation of Evi-1 Mutant Mice

(A) Schematic representation of Evi-1 isoforms. ZF1, zinc finger domain-1; ZF2, zinc finger domain-2; PR, PR domain.

(B) Schematic representation of gene targeting of the *Evi-1* gene. E, *Eco*RV; S, *Sph*I; neo/tk, PGK-neo/HSV-thymidine kinase positive selection cassette; DT-A, diphtheria toxin A chain negative selection cassette.

(C) Southern blot analysis of *Sph*I- (KO, knockout mice) or *Eco*RV- (cKO, conditional knockout mice) digested genomic tail DNA showing the predicted fragment-length polymorphism.

(D) Expression of Evi-1 and β-actin protein in *Evi-1*$^{+/+}$ and *Evi-1*$^{-/-}$ embryos. Lysates were prepared from mouse embryo fibroblast (MEF) cells from E14.5 embryos and were analyzed by western blotting using anti-Evi-1 antibody (C50E12). *Nonspecific band.

(E) Genotypes of litters obtained by intercrossing *Evi-1*$^{+/-}$.

(F) Gross appearance of embryos at E16.5. The *Evi-1*$^{-/-}$ embryo showed hemorrhaging with the yolk sac exhibiting severe anemia and defective large-vessel development.

Evi-1b might contribute to the complex phenotype observed in these mice.

In contrast to the established role of Evi-1 in leukemia development, the role of Evi-1 in normal hematopoiesis has been poorly understood. Recently, it was reported that *Evi-1* is predominantly expressed in both embryonic and adult hematopoietic stem cells (HSCs), and development of definitive HSCs in the para-aortic splanchnopleural (P-Sp) region was severely impaired in *Evi-1* mutant embryos (Yuasa et al., 2005). In addition, several studies have shown that retroviral vector integration at the *Evi-1* locus can be related to long-term in vivo clonal dominance without necessarily resulting in malignant transformation in mice (Kustikova et al., 2005), nonhuman primates (Calmels et al., 2005), and humans (Ott et al., 2006). These findings suggest that Evi-1 has a role in the regulation of HSCs; however, further functional analysis of Evi-1 has been hampered because of the embryonic lethality of the *Evi-1* mutant mice.

To further investigate the physiological role of Evi-1 in hematopoiesis, we created mutant mice in which exon 4 of the *Evi-1* gene can be deleted by the expression of Cre recombinase, as well as mice in which the same region was completely deleted. Using these mice, we here show that Evi-1 regulates proliferative capacity of HSCs in a dose-dependent manner both during embryogenesis and in adults. We further demonstrate that Evi-1 is also required for proliferation of transformed leukemic cells, and we provide candidate target genes of Evi-1 shared in HSCs and leukemic cells.

RESULTS

Generation of Evi-1 Mutant Mice

The mutant mice of Evi-1 were previously generated by disrupting exon 7 of the *Evi-1* gene (Hoyt et al., 1997); however, these mice still retain the Evi-1b, and they lack the longer isoforms of Evi-1 (Evi-1a and Evi-1c). Therefore, we targeted exon 4 of the *Evi-1* gene that is conserved in all of the known isoforms (Figure 1A) and created mutant mice carrying deleted (Evi-1$^-$) or loxP-flanked (Evi-1^f) alleles (Figure 1B). Germline transmission was confirmed by Southern blot analysis of tail DNA (Figure 1C). Disruption of exon 4 of Evi-1 was confirmed by PCR and northern blotting using RNA in embryos and by sequencing the amplified PCR product of *Evi-1*$^{-/-}$ embryo (Figures S1, S2, S3, and S4 available online). Immunoblotting of *Evi-1*$^{-/-}$ embryo using three different antibodies confirmed that all three isoforms of Evi-1 protein are absent in homozygous embryos (Figures 1D and S5).

C57BL/6 Mice Lacking Three Isoforms of Evi-1 Died between E13.5 and E16.5

First, we analyzed our conventional Evi-1 knockout mice. Newly generated *Evi-1*$^{+/-}$ mice were born and were fertile, exhibiting no morphological abnormalities. In contrast, *Evi-1*$^{-/-}$ pups were not seen. To identify the stage of embryonic development at which the Evi-1 mutation is lethal, E9.5–18.5 embryos were analyzed for their genotype (Figure 1E). Surprisingly, our *Evi-1*$^{-/-}$ mice were alive with normal appearance at E10.5, when the previously developed *Evi-1* mutant mice died. After E13.5, many *Evi-1*$^{-/-}$ embryos exhibited hemorrhaging and subcutaneous edema, with the yolk sacs showing severe anemia and defective large-vessel development (Figure 1F). Some *Evi-1*$^{-/-}$ embryos survived as long as E16.5 with comparable body size to wild-type littermates, but no viable *Evi-1*$^{-/-}$ fetuses were detected after E18.5. Thus, our *Evi-1*$^{-/-}$ mice lacking three isoforms of *Evi-1* survived slightly longer than the prior *Evi-1* mutant mice, but they died between E13.5 and E16.5.

Decreased Hematopoietic Stem/Progenitor Cells in *Evi-1*-Deficient Embryos

To assess the role of Evi-1 in hematopoiesis, we first examined the capacity of definitive hematopoiesis in *Evi-1*$^{-/-}$ embryos, which occurs in the P-Sp region at E9.5, using an in vitro P-Sp explant/OP9 stromal cell coculture system (Goyama et al., 2004). Consistent with the findings obtained for the prior *Evi-1* mutant mice (Yuasa et al., 2005), the number of HSCs in the *Evi-1*$^{-/-}$ P-Sp cultures was significantly decreased in comparison to the number of HSCs in the wild-type controls (Figure 2A). We next assessed fetal liver (FL) hematopoiesis in *Evi-1*$^{+/-}$ and *Evi-1*$^{-/-}$ mice. The *Evi-1*$^{-/-}$ FL contained nucleated erythrocytes, granulocytes, and B-lymphocytes and was morphologically indistinguishable from the wild-type FL (Figures 2B and S6). However, the population of lineage$^-$, c-Kit$^+$, Sca-1$^+$ cells (LSK cells) or lineage$^-$, c-Kit$^+$, CD34$^+$ cells, which enriches hematopoietic stem/progenitor cells, was severely reduced in *Evi-1*$^{-/-}$ mice. The *Evi-1*$^{+/-}$ FL showed an intermediated phenotype (Figure 2B). The total number of colony-forming cells (CFCs), especially the number of mixed colonies, in *Evi-1*$^{-/-}$ FL cells was also severely decreased (Figure 2C). Together, these results suggest that Evi-1 deletion causes severe reduction in hematopoietic stem/progenitor cells but is compatible with differentiation of progenitors once they are formed.

Defective HSC Activity in *Evi-1*-Deficient Embryos

To determine whether *Evi-1*$^{-/-}$ embryos possess functional HSCs, we tested the ability of *Evi-1*$^{-/-}$ FL cells to reconstitute the hematopoietic system of recipient mice. FL cells (2×10^6 cells) from E14.5 wild-type or *Evi-1*$^{-/-}$ embryos were injected into lethally irradiated (9.5 Gy) recipient mice. All recipients receiving wild-type FL cells survived and remained healthy for at least 1 month; however, no recipients receiving donor cells from *Evi-1*$^{-/-}$ embryos survived beyond 2 weeks (Figure 2D). We further performed the competitive reconstitution assay. FL cells (1×10^6 cells) from wild-type or *Evi-1*$^{-/-}$ (Ly5.2) embryos were injected into lethally irradiated recipient mice (Ly5.1) together with 2×10^5 competitor bone marrow (BM) cells from wild-type mice (Ly5.1). *Evi-1*$^{-/-}$ cells were not detected at all in the recipient mice either 4 or 16 weeks after transplantation. In contrast, wild-type FL cells reconstituted hematopoiesis of the recipients to a larger extent than competitor cells (Figures 2E and S7). Thus, Evi-1 is required for HSC activity to reconstitute the hematopoietic system in recipients.

Deletion of Evi-1 in Tie2$^+$ Cells Mimics Evi-1 Deficiency

Next, we crossed Evi-1$^{f/f}$ mice with Tie2-Cre mice (Li et al., 2006) to selectively disrupt Evi-1 function in Tie2$^+$ endothelial and hematopoietic stem/progenitor cells. Most of Tie2-Cre$^+$;Evi-1$^{f/f}$ embryos died around E13.5 to E16.5 with hemorrhage and/or subcutaneous edema, as *Evi-1*-deficient embryos do (Figures 3A and 3B). A few Tie2-Cre$^+$;Evi-1$^{f/f}$ mice were born alive and grew to adults (Figure 3A), but BM of these mice primarily

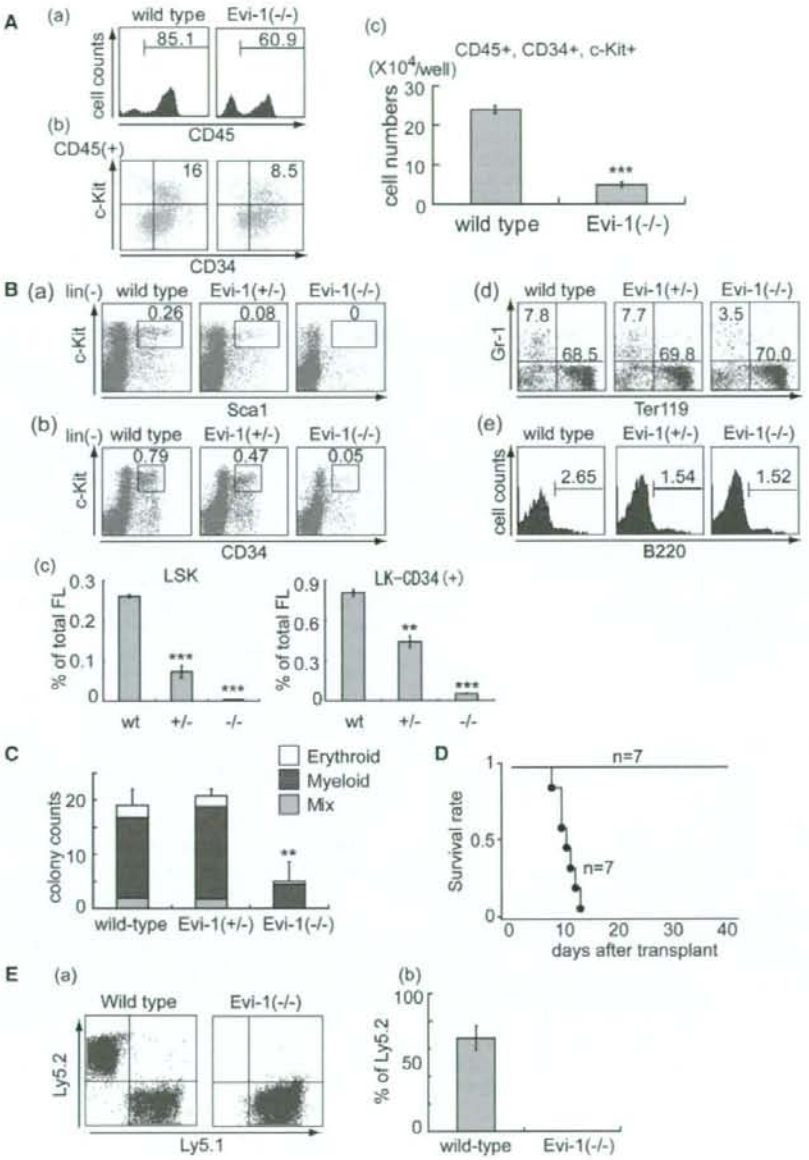

Figure 2. Decreased Hematopoietic Stem/Progenitor Cells in *Evi-1*$^{-/-}$ Embryos

(A) Flow cytometric profiles of the cells from the P-Sp cultures harvested after 5 days in culture. (Aa) CD45$^+$ cells in P-Sp culture were gated. (Ab) CD45$^+$ cells were examined for the expression of CD34 and c-Kit. (Ac) The numbers of CD45$^+$, CD34$^+$, c-Kit$^+$ hematopoietic stem/progenitor cells in P-Sp culture derived from wild-type or *Evi-1*$^{-/-}$ mice. n = 3. ***p = 0.0001.

(B) Flow cytometric profiles of wild-type, *Evi-1*$^{+/-}$, and *Evi-1*$^{-/-}$ littermate FL at E14.5. (Ba and Bb) Population of hematopoietic stem/progenitor cells. (Bc) Quantification of flow cytometric analysis. Data are mean ± SD from four mice. P values were calculated as compared with wild-type embryos. **p = 0.0043. ***p < 0.0001. (Bd) Population of myeloid and erythroid cells. (Be) Population of B-lymphocytes. Numbers of each panel represent percentages of the gated population in whole FL cells.

(C) CFCs in wild-type, *Evi-1*$^{+/-}$, and *Evi-1*$^{-/-}$ littermate FL cells. p values were calculated as compared with wild-type embryos. n = 4. **p = 0.0009.

(D) Survival curve of lethally irradiated recipients receiving either wild-type or *Evi-1*$^{-/-}$ FL cells.

(E) Competitive repopulation assays. (Ea) Flow cytometric analysis of peripheral blood cells at 4 weeks after transplantation show extensive contribution of wild-type FL cells (Ly5.2), but no detectable contribution of *Evi-1*$^{-/-}$ cells. (Eb) Cumulative data of donor contribution in peripheral blood of recipients 4 weeks after transplantation. n = 6. Data are mean ± SD.

A

				Tie2-Cre			
	Evi-1$^{+/+}$	Evi-1$^{f/+}$	Evi-1$^{f/f}$	Evi-1$^{+/+}$	Evi-1$^{f/+}$	Evi-1$^{f/f}$	total
E11.5	0	2	0	2	4	1	9
E12.5	2	3	1	5	3	3	17
E13.5	6	2	3	3	5	2	21
E14.5	1	3	0	0	3	2	9
E15.5	2	6	2	2	1	1	14
E16.5	1	3	2	3	2	1	12
E17.5	1	5	3	4	3	1	17
E18.5	1	2	0	2	2	0	7
Pups	22	25	15	19	15	3	96

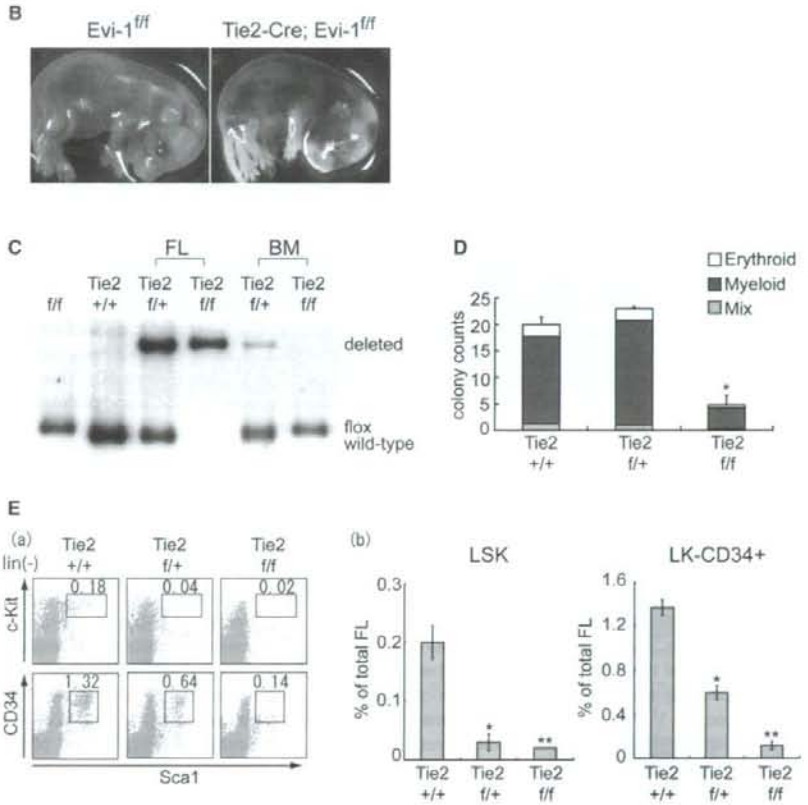

Figure 3. Selective Ablation of Evi-1 in Tie2$^+$ Cells

(A) Genotypes of litters obtained by intercrossing Tie2-Cre;Evi-1$^{f/+}$ and Evi-1$^{f/+}$ mice.

(B) Gross appearance of E16.5 fetuses. Tie2-Cre;Evi-1$^{f/f}$ embryo are edematic and show hemorrhaging.

(C) Southern blot genotyping of FL cells (E14.5) and BM cells (1 month after birth). Evi-1 was excised efficiently in E14.5 fetal liver cells of Tie2-Cre;Evi-1$^{f/f}$ embryos, but BM cells of the surviving Tie2-Cre;Evi-1$^{f/f}$ mice exclusively harbored nonexcised Evi-1 allele.

(D) CFCs in Tie2-Cre;*Evi-1*$^{+/+}$, Tie2-Cre;Evi-1$^{f/+}$, Tie2-Cre;Evi-1$^{f/f}$ littermate FL cells. p values were calculated as compared with Tie2-Cre;*Evi-1*$^{+/+}$ embryos. n = 2. $^*p = 0.0108$.

(E) (Ea) Population of hematopoietic stem/progenitors in Tie2-Cre;*Evi-1*$^{+/+}$, Tie2-Cre;Evi-1$^{f/+}$, Tie2-Cre;Evi-1$^{f/f}$ littermate FL cells (E14.5). Numbers of each panel represent percentages of the gated population in whole FL cells. (Eb) Quantification of flow cytometric analysis. Data are mean ± SD from two mice. p values were calculated as compared with Tie2-Cre;*Evi-1*$^{+/+}$ embryos. (LSK) $^*p = 0.0077$, $^{**}p = 0.0041$. (CD34$^+$-LK) $^*p = 0.0113$. $^{**}p = 0.002$.

consisted of cells that retain the nonexcised Evi-1^f allele (Figure 3C), indicating that hematopoiesis originated from cells that had escaped Cre-mediated excision. HSCs and CFCs were severely decreased in the FL of Tie2-Cre$^+$;Evi-1$^{f/f}$ embryos (Figures 3D, 3E, and S8). Thus, selective ablation of Evi-1 in Tie2$^+$ cells virtually reproduced all of the phenotypes of *Evi-1*$^{-/-}$ mice,

suggesting that Evi-1 function is required in Tie2$^+$ cells for early development and proliferation of HSCs.

Evi-1 Is Essential for Proliferation/Maintenance of Adult BM HSCs

To assess a role of Evi-1 in adult hematopoiesis, we then crossed Evi-1$^{f/f}$ mice with Mx-Cre transgenic mice, in which a high level of Cre recombinase is produced by treatment with the interferon inducer pI-pC, leading to recombination in hematopoietic cells of all lineages. Injection of pI-pC did not cause significant differences in white blood cell (WBC) counts or hemoglobin levels among the Mx-Cre;Evi-1$^{f/f}$ (*Evi-1*-excised), Mx-Cre;*Evi-1*$^{+/+}$, and Evi-1$^{f/f}$ mice, and the platelet counts in the *Evi-1*-excised mice modestly declined compared with those in control mice 4 weeks after pI-pC injection (Figure 4A). We next examined the effect of Evi-1 deletion in various hematopoietic cell populations. By 4 weeks after pI-pC injection, *Evi-1*-excised mice exhibited significant decrease in the frequency of HSCs and CFCs compared with control mice (Figures 4B and S9). In contrast, the frequencies of mature myeloid cells (Gr-1$^+$ or Mac-1$^+$ cells), B-lymphocytes (B220$^+$ cells), and T-lymphocytes (CD3$^+$, CD4$^+$, or CD8$^+$ cells) did not appear to be affected (Figure S10) in spite of the efficient excision of *Evi-1* alleles in a majority of these cells (Figure 4C, upper panel). Interestingly, by 12 weeks after pI-pC injection, cells in all hematopoietic populations contained primarily the nonexcised Evi-1^f allele (Figure 4C, lower panel). These results indicate that HSCs can not maintain hematopoiesis in the absence of Evi-1, and it is likely that a small fraction of HSCs that escaped Cre-mediated Evi-1 excision expand and predominate over *Evi-1*-deficient HSCs.

We further assessed a role of Evi-1 for the hematopoietic reconstitution in BM progenitors using Cre-encoding retroviruses. BM progenitors were harvested from wild-type (Ly5.2) or Evi-1$^{f/f}$ (Ly5.2) mice and then infected with GFP (control) or Cre-GFP expressing retrovirus. Evi-1 is completely deleted only in the GFP$^+$, Cre-transduced fraction of Evi-1$^{f/f}$ BM progenitors (Figure 4D). We then injected these progenitors into sublethally irradiated (6.5 Gy) recipient mice (Ly5.1) and assessed the frequency of GFP$^+$ fraction in donor (Ly5.2) cells 2 weeks after transplantation. The infection efficiency among all three groups was similar before transplantation. Remarkably, we found a profound loss of GFP$^+$ cells in Cre-transduced Evi-1$^{f/f}$ BM progenitors after transplantation, although a modest Cre-induced stasis was observed in wild-type BM progenitors (Figure 4D). Taken together, these results suggest that Evi-1 is indispensable for proliferation/maintenance of adult BM HSCs, yet it is dispensable for differentiation into myeloid, erythroid, and lymphoid lines.

Haploinsufficiency of Evi-1 Perturbs Adult HSC Homeostasis

We then analyzed hematopoiesis of *Evi-1*$^{+/-}$ mice that survive through adulthood without overt abnormalities. Mature blood cell counts in peripheral blood of *Evi-1*$^{+/-}$ mice were comparable to those of wild-type mice (Figure S11). However, *Evi-1*$^{+/-}$ mice had a lower abundance of LSK and CD34$^-$LSK cells, which include short-term and long-term HSCs (Figure 5A). Therefore, we evaluated HSC function by testing the ability of *Evi-1*$^{+/-}$ BM cells to competitively repopulate the adult hematopoietic compartment in lethally irradiated recipient mice. BM cells from *Evi-1*$^{+/-}$ (Ly5.2) mice or wild-type littermates (Ly5.2) were transplanted into lethally irradiated Ly5.1 mice together with wild-type competitor Ly5.1 BM cells at a ratio of 1:1 or 1:10 of test cells to competitor cells. The average contribution of *Evi-1*$^{+/-}$ donor BM cells to total peripheral blood cells was lower than that of wild-type controls at 4 and 16 weeks after transplantation (Figure 5B). These results, together with the observation that *Evi-1*$^{+/-}$ FL had a reduced number of HSCs, suggest a gene dosage requirement for Evi-1 in the regulation of HSCs.

Delayed Hematopoietic Recovery after 5FU Treatment in *Evi-1*$^{+/-}$ and *Evi-1*-Excised Mice

To assess the effect of Evi-1 dose in the kinetics of hematopoietic recovery after myelosuppressive treatment, we administered a single dose of 5FU to wild-type and *Evi-1*$^{+/-}$ mice and serially followed peripheral blood counts. As shown in Figure 5C, *Evi-1*$^{+/-}$ mice showed a significant delay in the platelet recovery. We performed the same experiment using Mx-Cre;Evi-1$^{f/f}$, Mx-Cre;*Evi-1*$^{+/+}$, and Evi-1$^{f/f}$ mice 7 days after pI-pC injection and also found that platelet recovery was significantly delayed in *Evi-1*-excised mice (Figure 5C). These results indicate that Evi-1 has a specific role in platelet formation. Alternatively, perturbation of HSC compartment in *Evi-1*$^{+/-}$ and *Evi-1*-excised mice may have a stronger influence on platelet recovery than on the recovery of other lineages. The recovery of HSCs after 5FU administration in *Evi-1*-excised mice was also delayed, and the recovered HSCs in *Evi-1*-excised mice possessed primarily the nonexcised Evi-1^f allele (Figure 5D). Thus, Evi-1 is required for the efficient recovery of HSCs and platelets after myelosuppressive treatment.

Consequences of Evi-1 Deletion on Cell Viability and Proliferation

To characterize the defective proliferation capacity of hematopoietic stem/progenitors in *Evi-1*-excised mice, we assessed proliferation in vitro using a culture system that expands BM HSCs (Zhang and Lodish, 2005). BM progenitors derived from control (Evi-1$^{f/f}$) or *Evi-1*-excised (Mx-Cre;Evi-1$^{f/f}$) mice were cultured in serum-free medium containing SCF, TPO, IGF2, and FGF-1. We found that *Evi-1*-excised progenitors exhibited reduced proliferation relative to controls (Figure 6A). Cell-cycle and apoptosis analysis at day 15 of culture revealed a significant decrease in the proportion of S/G2/M phase cells and an increase in the percentage of Annexin-V-positive cells for *Evi-1*-excised cells (Figures S12 and S13). Accelerated apoptosis and impaired cell cycling will explain the attenuated proliferation of *Evi-1*-excised cells in this culture condition. We then excised Evi-1 in vitro using Cre-encoding retroviruses. BM progenitors were harvested from wild-type or Evi-1$^{f/f}$ mice and infected with GFP (control) or Cre-GFP-expressing retroviruses. These progenitors were cultured in the condition as described above and assessed the frequency of GFP$^+$ fraction every 5 days. This approach also revealed reduced proliferation of GFP$^+$ cells in Cre-transduced Evi-1$^{f/f}$ (*Evi-1*-excised) progenitors (Figures 6B and S14). Taken together, we concluded that Evi-1 is required for sustaining cytokine-dependent proliferation of hematopoietic stem/progenitors.

We next assessed in vivo cell-cycle distribution of FL or BM cells derived from control (Evi-1$^{f/f}$) or *Evi-1*-excised (Mx-Cre;

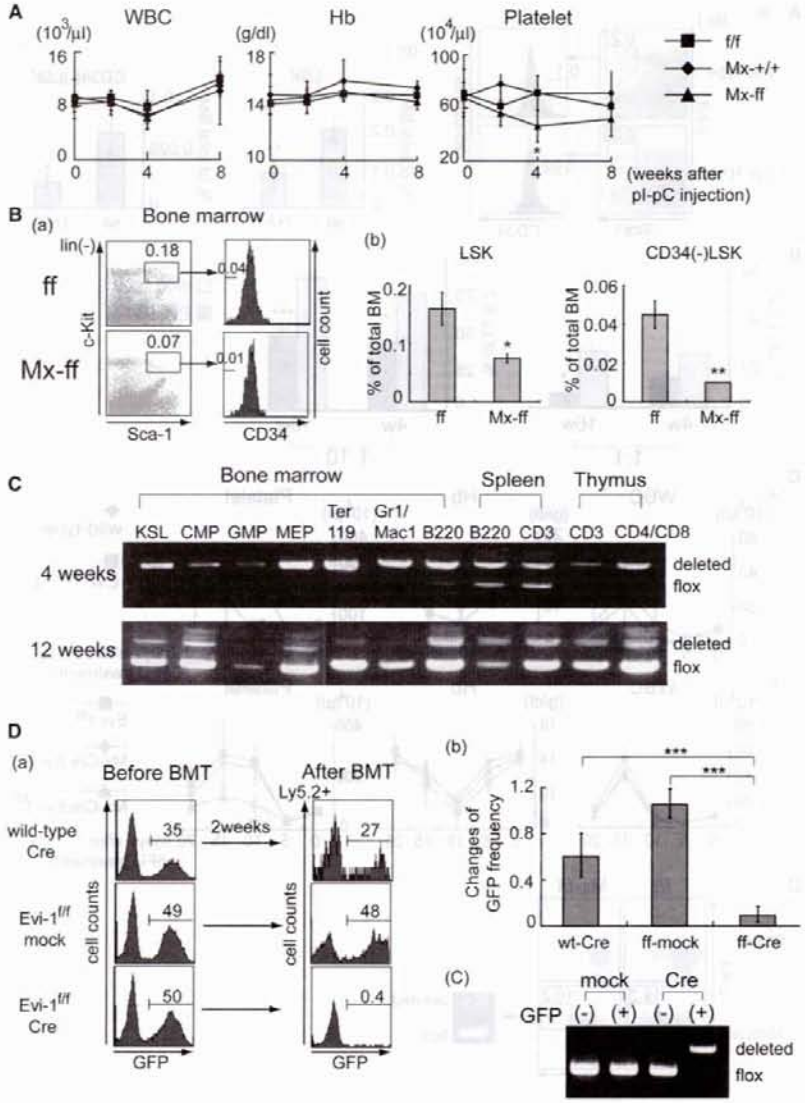

Figure 4. Disruption of Evi-1 in Adult Hematopoiesis

(A) Peripheral blood cell counts of Mx-Cre;*Evi-1*$^{+/+}$, Evi-1$^{f/f}$, and Mx-Cre;Evi-1$^{f/f}$ mice injected with pI-pC on weeks 0, 4, and 8. Results are shown as mean ± SD from three (controls) to eight (Mx-Cre;Evi-1$^{f/f}$) mice. p values were calculated as compared with controls. *p = 0.0004.

(B) Flow cytometric analysis of Evi-1$^{f/f}$ or Mx-Cre;Evi-1$^{f/f}$ mice 4 weeks after pI-pC injection. (Ba) Population of HSCs in the BM. Numbers of each panel represent percentages of the gated population in whole BM. (Bb) Quantification of flow cytometric analysis. n = 3. Data are mean ± SD. *p = 0.015. **p = 0.0031.

(C) PCR genotyping of cells from various hematopoietic populations of Mx-Cre;Evi-1$^{f/f}$ mice 4 weeks (upper panel) and 12 weeks (lower panel) after pI-pC injection. Efficient excision of *Evi-1* was observed at 4 weeks, but cells in all populations at 12 weeks primarily harbored nonexcised *Evi-1* allele.

(D) (Da) Infection efficiencies before transplantation were compatible among three groups, but GFP$^+$ fraction in Cre-transduced Evi-1^{ff} BM cells (*Evi-1*-excised cells) disappeared after transplantation. (Db) Relative ratios of GFP$^+$ fraction in Ly5.2 donor cells after transplantation compared with those before transplantation. Data are shown as mean ± SD from three independent experiments. Each group contains six mice. ***p < 0.0001. (Dc) PCR analysis of flanked *Evi-1* alleles in control and Cre-transduced BM cells. The flanked *Evi-1* alleles became undetectable in GFP$^+$, Cre-transduced Evi-1$^{f/f}$ BM cells.

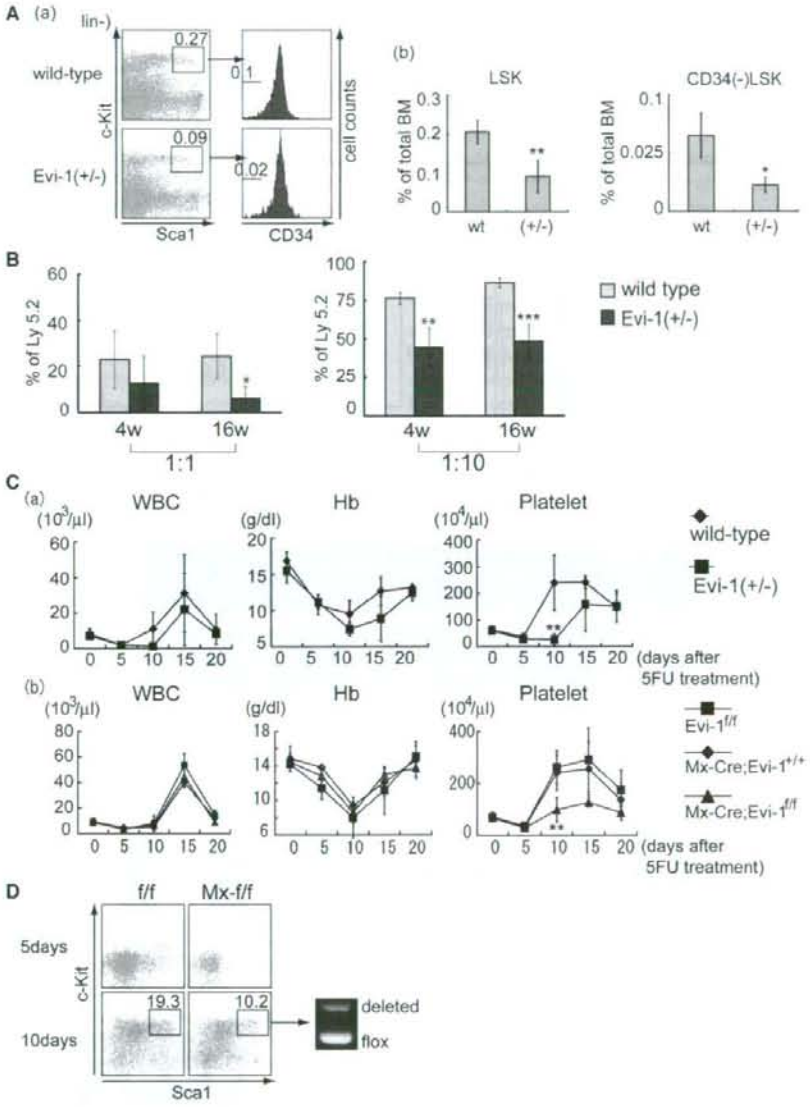

Figure 5. Defective HSC Activity and Delayed Hematopoietic Recovery in *Evi-1*$^{+/-}$ and *Evi-1*-Excised Mice

(A) (Aa) *Evi-1*$^{+/-}$ BM exhibited significant decrease in the size of the short-term (ST)-HSC (lin$^-$, Sca-1$^+$, c-Kit$^+$) and long-term (LT)-HSC (CD34$^-$, lin$^-$, Sca-1$^+$, c-Kit$^+$) compartments. (Ab) Quantification of flow cytometric analysis on the size of ST- and LT-HSCs of wild-type and *Evi-1*$^{+/-}$ mice. n = 4. Data are mean ± SD *p = 0.0056. **p = 0.0041.

(B) Competitive transplantation reveals diminished repopulating ability of *Evi-1*$^{+/-}$ BM. n = 4. Data are shown as mean ± SD. 1:1, *p = 0.03242. 1:10, **p = 0.0028, ***p = 0.0005.

(C) Peripheral blood cell recovery after 5FU treatment was followed by serial peripheral blood count monitoring of mice. (Ca) Wild-type and *Evi-1*$^{+/-}$ mice. n = 4. **p = 0.0091. (Cb) Mx-Cre;*Evi-1*$^{+/+}$, Evi-1$^{f/f}$, and Mx-Cre;Evi-1$^{f/f}$ mice 7 days after induced deletion of the floxed genes. p values were calculated as compared with controls. n = 4. **p = 0.0012.

(D) HSC recovery after 5FU treatment of Evi-1$^{f/f}$ and Mx-Cre;Evi-1$^{f/f}$ mice. HSC recovery was modestly delayed in *Evi-1*-excised mice, and re-emerging HSCs had primarily harbored nonexcised *Evi-1* allele. Similar results were obtained in three independent experiments.

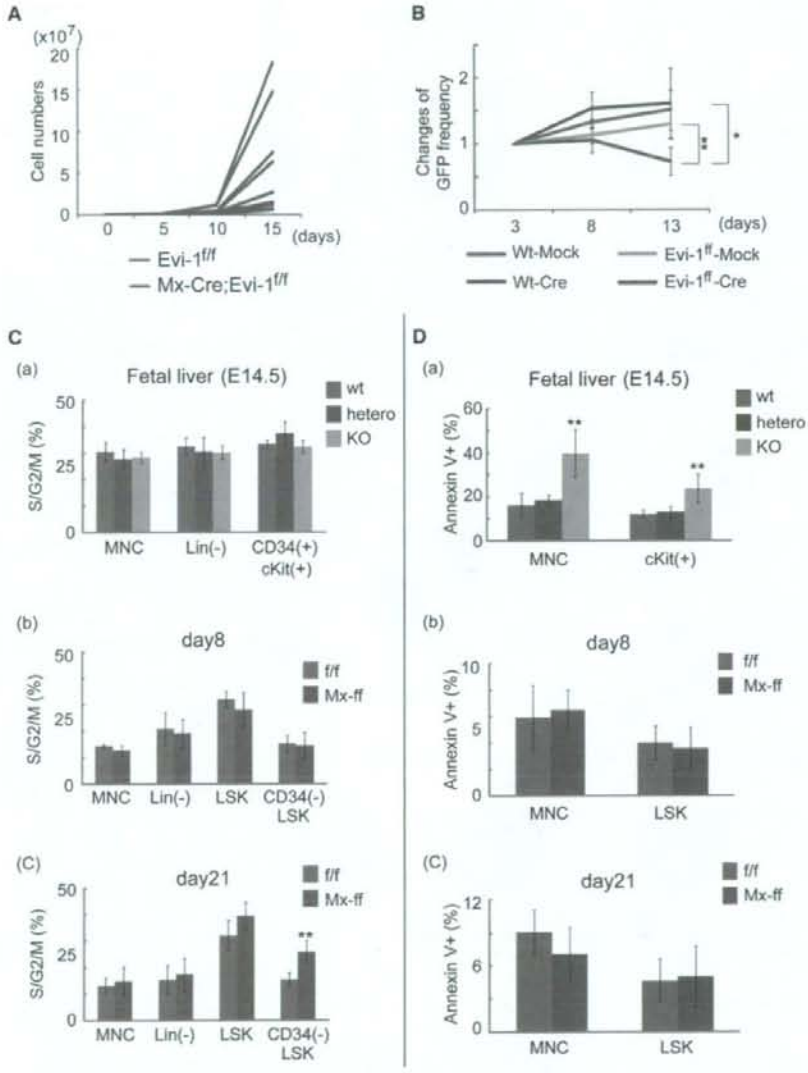

Figure 6. Effects of Evi-1 Deletion on Cell Death and Proliferation

(A) Lineage$^-$, c-Kit$^+$ cells were purified from Evi-1$^{f/f}$ or Mx-Cre; Evi-1$^{f/f}$ mice 3–4 weeks after Cre induction. Cells were cultured in liquid medium containing SCF, TPO, IGF-2, and FGF-1. Total cell numbers were monitored every 5 days. Five independent experiments were performed in each group.

(B) BM progenitors derived from wild-type or Evi-1$^{f/f}$ mice were transduced with GFP or Cre-GFP retrovirus and were cultured as in (A). The frequency of GFP$^+$ fraction was assessed every 5 days. Four or five independent experiments were performed in each group. *p = 0.0108. **p = 0.0061.

(C) Cell-cycle status was assessed in various hematopoietic populations of E14.5 FL cells (Ca), BM cells at day 8 post Cre induction (Cb), and BM cells at day 21 post Cre induction (Cc). *Evi-1*-excised FL cells and BM cells at day 8 post Cre induction exhibited normal cell-cycle distribution relative to littermate controls, but *Evi-1*-excised CD34$^-$ LSK cells at day 21 post Cre induction showed an increased frequency of S/G2/M phase cells. **p = 0.0015.

(D) Apoptosis was assessed using Annexin-V staining. (Da) *Evi-1*-excised FL cells exhibited an increased frequency of Annexin-V$^+$ cells. (Db and Dc) *Evi-1*-excised BM cells exhibited normal frequency of apoptotic cells both at days 8 and 21 after Cre induction. **p = 0.004 (MNC). p = 0.0021 (c-Kit[+]). MNC, mononuclear cells; Lin, lineage.

Evi-1$^{f/f}$) mice. We found a significant increase in S/G2/M phase CD34$^-$ LSK cells in *Evi-1*-excised BM 21 days after Cre induction. In contrast, no difference in cell-cycle distribution was detected in *Evi-1*-excised BM cells immediately after Cre induction (at day 8). Furthermore, Evi-1 deletion had no effect on the cell-cycle distribution of FL cells (Figure 6C). Therefore, the increased

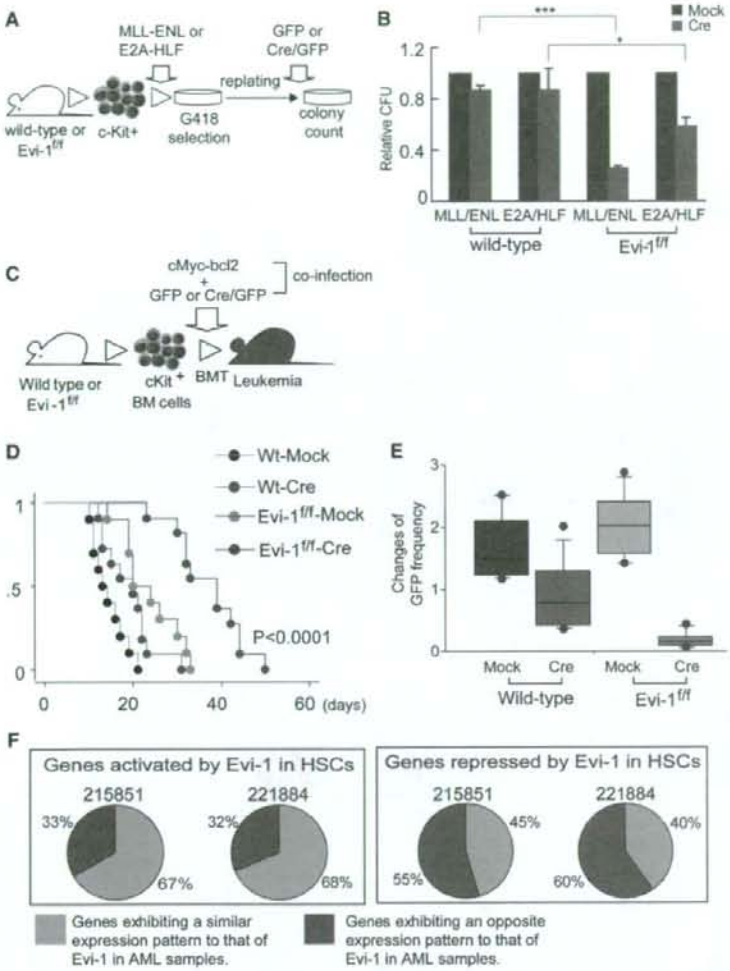

Figure 7. Evi-1 Determines Proliferative Capacity of Transformed Leukemic Cells

(A) Schematic representation of the following experiments. BM progenitors from wild-type or Evi-$1^{f/f}$ mice were transduced with MLL/ENL or E2A/HLF oncogenes. Immortalized cells from the third to fifth round of in vitro plating were subsequently transduced with either GFP- or Cre-GFP-expressing retrovirus. GFP$^+$ cells were sorted, and then relative clonogenic activity was assessed in the additional round of plating.

(B) Relative numbers of colonies generated by Cre-transduced cells compared with GFP-transduced cells. Deletion of Evi-1 significantly attenuated clonogenic activities of MLL/ENL and E2A/HLF-transformed cells to 28% and 58% of the controls. Data are shown as mean ± SD from three (MLL/ENL) and four (E2A/HLF) independent experiments. *p = 0.0322, ***p = 0.0001.

(C) Schematic representation of the following experiments. BM progenitors from wild-type or Evi-$1^{f/f}$ mice were transduced with cMyc-bcl2 in combination with GFP or Cre-GFP. Infected progenitors were transplanted into recipients.

(D) Survival curves of mice transplanted with wild-type or Evi-$1^{f/f}$ progenitors transduced by cMyc-bcl2 + GFP or Cre-GFP. Each group contains 10 or 11 mice.

(E) Relative ratios of GFP$^+$ fraction in leukemic cells after transplantation compared with those before transplantation. Peripheral blood cells were isolated from moribund mice, and the frequencies of the GFP$^+$ cells were assessed. Data are shown as a boxplot.

(F) Expression patterns of putative target genes of Evi-1 in cases with AML. Areas of each circular graph represent the percentages of genes exhibiting a similar or opposite expression pattern to that of Evi-1 in AML samples. Results are depicted as for two independent probes (215851 and 221884) used for evaluation of Evi-1 expression.

number of cycling *Evi-1*-excised HSCs at day 21 is probably due to the depletion of quiescent BM HSCs rather than the direct effect of Evi-1 deletion. We then assessed apoptosis in FL or BM cells by Annexin-V-binding to cell surface. Evi-1 deletion significantly increased the rate of cell death in FL cells. However, no significant difference was noted in the percentage of Annexin-V-positive cells in control or *Evi-1*-excised BM cells (Figure 6D). Therefore, the increased cell death would contribute to the defective proliferation of *Evi-1*-excised FL cells but did not account for the homeostasis defects of *Evi-1*-excised BM HSCs. Thus, the effects of Evi-1 deletion on cell cycling and viability in vivo vary in a context-dependent manner.

Evi-1 Is Required for Efficient Propagation of Transformed Leukemic Cells

Next, we evaluated a role for Evi-1 in myeloid transformation. MLL/ENL (ME) and E2A/HLF (EH) are chimeric genes generated in t(11;19) and t(17;19) leukemias, respectively, both of which are known to transform murine BM cells by distinct molecular mechanisms, resulting in sustained colony formation in the serial replating assay (Ayton and Cleary, 2003; Smith et al., 2002). BM progenitors were harvested from wild-type or Evi-$1^{f/f}$ mice and then transduced with ME or EH. After establishment of sustained clonogenic activity following more than three rounds of replating in methylcellulose medium, the cells were transduced with GFP or Cre-GFP-expressing retroviruses. Then, GFP$^+$ cells were sorted and subjected to another round of replating to evaluate relative clonogenic activity (Figure 7A). Disruption of Evi-1 in ME-transformed progenitors caused significant reduction in colony numbers to about 30% of the control, whereas Cre expression in ME-transformed wild-type progenitors resulted in marginal decrease of clonogenic activity. Evi-1 deletion also modestly reduced clonogenic activity in EH-transformed cells to about 60% of the control (Figure 7B).

We next examined a role for Evi-1 in in vivo leukemia development using transplantation of the cells transduced by cMyc-bcl2

into sublethally irradiated syngeneic mice. This murine leukemia model is useful for evaluating the in vivo effects of Evi-1 deletion on the leukemogenetic activity because these mice developed leukemia with very short latencies. BM progenitors purified from wild-type or Evi-$1^{f/f}$ mice were cotransduced with cMyc-bcl2 together with GFP or Cre-GFP-expressing retroviruses. We then injected these progenitors (1×10^6) into recipient mice and assessed their survival (Figure 7C). All the recipient mice developed leukemia as described previously (Luo et al., 2005; Figure S15); however, the mice transplanted with *Evi-1*-excised cells died with significantly longer latencies (Figure 7D). Furthermore, we found significant loss of GFP^+ cells in the peripheral blood of the leukemic mice transplanted with cMyc-bcl2- and Cre-transduced Evi-$1^{f/f}$ (*Evi-1*-excised) progenitors, suggesting impaired contribution of *Evi-1*-excised cells to leukemia, although a modest Cre-induced stasis was observed as for wild-type progenitors (Figure 7E). We also used the two-step transplantation model to assess the effect of Evi-1 deletion on the maintenance of leukemia. We first transplanted wild-type or Evi-$1^{f/f}$ progenitors transduced with cMyc-bcl2 into recipients. Leukemic cells were then isolated from the spleens of moribund primary cMyc-Bcl2 mice, and the cells were transduced with GFP or Cre-GFP-expressing retroviruses. Then, the GFP^+ cells were sorted and transplanted into secondary recipients to evaluate the leukemogenic activity (Figure S16). This approach again demonstrated that the mice transplanted with *Evi-1*-excised leukemic cells died with significantly longer latencies (Figure S17). Thus, Evi-1 is required for efficient propagation of transformed leukemic cells both in vitro and in vivo.

Putative Target Genes of Evi-1 in HSCs and AML Samples

To identify the common target genes of Evi-1 shared in HSCs and leukemic cells, we first carried out genome-wide transcriptional analysis using GFP or Cre-GFP-infected Evi-$1^{f/f}$ HSCs. LSK cells derived from Evi-$1^{f/f}$ mice were transduced with GFP or Cre-GFP-expressing retroviruses, and GFP^+ cells were sorted. Evi-1 deletion in Cre-GFP-transduced cells was confirmed by PCR (Figure S18). Linear amplification of RNA obtained from GFP^+ cells and subsequent gene-expression profiling identified 378 downregulated and 446 upregulated genes in *Evi-1*-deleted HSCs. Transcripts were considered upregulated or downregulated if the change in transcript level as a multiple of the control was >1.2. We then assessed the correlation between expression of Evi-1 and these potential target genes in AML samples using gene-expression data of 285 individuals with AML (Valk et al., 2004; Figure S19). We found that expression of the genes activated by Evi-1 in HSCs tends to coincide with that of Evi-1 in AML samples, whereas many of the genes repressed by Evi-1 in HSCs showed an expression pattern opposite to that of Evi-1 in AML (Figure 7F). Thus, our approach revealed the existence of the common regulatory pathway underlying Evi-1-mediated hematopoiesis and leukemogenesis and provides putative target genes of Evi-1 in both HSCs and leukemic cells. The potential Evi-1 target genes include genes whose expression is decreased in the *Evi-1*$^{-/-}$ P-Sp region (Gata1, Gata2, and Angpt1) (Yuasa et al., 2005), genes involved in the regulation of HSCs (Gata2, Angpt1, Mpl, Jag2, Pbx1, and Setbp1), and genes related to platelet formation (Gata1, Mpl, Itga2b, and Itgb3) (Tables S1 and S2). We evaluated the expression levels of some of the putative target genes of Evi-1 in LSK cells transduced with GFP or Cre-GFP using quantitative PCR method, and we found that they showed a similar tendency to the results obtained by the microarray analysis (Figure S20).

DISCUSSION

Although Evi-1 has been recognized as a crucial gene that promotes leukemogenesis, a physiological role of Evi-1 in vivo, particularly in terms of adult hematopoiesis, is poorly understood. In this study, we generated Evi-1 mutant mice and showed that Evi-1 is a common regulator essential for proliferation of hematopoietic stem/progenitor cells both during fetal development and in adults. Evi-1 function is required for establishment of definitive HSCs in $Tie2^+$ cells of developing embryos. Furthermore, *Evi-1*$^{+/-}$ mice exhibited the intermediate phenotype as for the number of HSCs, as well as hematopoietic reconstitution activity of the BM cells, suggesting a gene dosage requirement for Evi-1 in the regulation of HSCs. We also found that the platelet counts modestly declined in *Evi-1*-excised mice, and platelet recovery after the myelosuppressive treatment was significantly delayed in *Evi-1*$^{+/-}$ and *Evi-1*-excised mice. Although the underlying mechanism responsible for this defective platelet formation remains to be identified, this phenotype may reflect the clinical feature of elevated platelet counts in AML/MDS cases carrying 3q26 rearrangements.

The *Evi-1*$^{-/-}$ mice we have created survived longer than the previously developed *Evi-1* mutant mice. In the prior *Evi-1* mutant mice, the expression of Evi-1b (shorter isoform) is unaffected. In addition, the previous Evi-1 knockout was established with ES-D3 cells with chimeras subsequently mated to CF-1 mice. Therefore, both the presence of Evi-1b in the prior *Evi-1* mutant mice and dissimilar genetic backgrounds may contribute to the different stages of death.

An emerging concept in the field of cancer biology is that a rare population of "cancer stem cells" exists among the heterogeneous group of cancer cells (Bonnet and Dick, 1997). Cancer stem cells have the abilities to self-renew and differentiate into multiple cell types, and these cells persist in tumors as a distinct population that likely causes disease relapse. Therefore, elimination of the cancer stem cell compartment is necessary and potentially sufficient for cure of the cancer. Several factors that govern the fate of adult stem cells also play a significant role in the regulation of cancer stem cells, such as Wnt, Notch, hedgehog, and Bmi-1 (Huntly and Gilliland, 2005; Lessard and Sauvageau, 2003). Of note, retrovirus-induced Evi-1 activation in hematopoietic cells leads to long-term in vivo clonal dominance of the infected cells (Calmels et al., 2005; Kustikova et al., 2005; Ott et al., 2006), and elevated expression of Evi-1 is associated with poor treatment outcomes in leukemia patients (Barjesteh van Waalwijk van Doorn-Khosrovani et al., 2003; Valk et al., 2004). Therefore, together with the findings in this report, we hypothesized that activation of Evi-1 enhances proliferation/survival of leukemia stem cells and, thus, confers drug resistance on various types of leukemia. In support of this is our observation that Evi-1 deletion in transformed leukemic cells leads to significant loss of their proliferative activity both in vitro and in vivo. Therefore, it is tempting to speculate that Evi-1 induces leukemia

development with cooperative oncogenes by enhancing self-renewing capacity in leukemic cells. Consequently, therapies designed to target Evi-1 will be an attractive option in the treatment of leukemia patients, especially in the treatment of those with a poor prognosis.

The presence of zinc fingers that are able to bind to specific sequences of DNA suggests that Evi-1 is a transcriptional regulator; however, target genes of Evi-1 have been poorly identified thus far. Here, we identified candidate Evi-1 target genes using gene-expression-profiling analysis in HSCs combined with the gene-expression data of AML samples. Our analysis revealed the existence of common target genes of Evi-1 in HSCs and leukemic cells. Notably, many genes involved in the HSC regulation, including *Gata2*, *Angpt1*, *Mpl*, *Jag2*, *Pbx1*, and *Setbp1*, are activated by Evi-1, implying that Evi-1 acts as a key regulator in HSCs and leukemic cells. Although it has yet to be determined whether these are primary targets of Evi-1, these data provide a starting point for further studies to uncover the underlying mechanisms for Evi-1-mediated hematopoiesis and leukemogenesis.

Finally, the functions of Evi-1 that we identified in the current study provide an insight into homeostasis and malignant transformation of various types of organs other than the hematopoietic system. Evi-1 is expressed in several other organs, including kidney and ovary (Morishita et al., 1990). Furthermore, aberrant expression of Evi-1 has been frequently found in a variety of solid tumors (Sugita et al., 2000). Thus, Evi-1 may play an important role in stem cell regulation and cancer development in a broad spectrum of tissues.

EXPERIMENTAL PROCEDURES

Mice

Evi-1 mutant mice were generated as described in the Supplemental Experimental Procedures. For conditional deletion of Evi-1 in vivo, mice possessing the Evi-1^f allele were mated to Tie2-cre or Mx-cre transgenic mice. Mx-cre expression was induced by intraperitoneally injecting 500 μg of pIpC, on 3 alternate days, into 6- to 8-week-old mice. Times after pI-pC injection are counted from the first day of injection. Competitive repopulation assay was performed using the Ly5 congenic mouse system. Mice were kept at the Animal Center for Biomedical Research, University of Tokyo, according to institutional guidelines.

Flow Cytometric Analysis

A list of antibodies is provided in the Supplemental Experimental Procedures. Cells were sorted with a FACSAria, and analysis was performed on FACSCaliber or LSRII (BD Biosciences). To analyze the cell-cycle status, cells were first stained with lineage and stem/progenitor markers, followed by staining with 10 ng/ml Hoechst 33342 at 37°C for 75 min. Apoptosis was assayed by staining cells with lineage and stem/progenitor markers, followed by Annexin-V and propidium iodide (PI) staining.

P-Sp Culture

P-Sp culture was performed as described previously (Goyama et al., 2004).

Colony-Forming Assay

Colony-forming assay was performed in MethoCult GF M3434 (Stem Cell Technologies) with 2×10^4 FL or BM cells and scored for mixed, myeloid, erythroid colony formation at 7 days.

Retrovirus Production

To produce oncoprotein-expressing retrovirus, Plat-E packaging cells (Kitamura et al., 2003) were transiently transfected with retroviral constructs (see the Supplemental Experimental Procedures), as described previously (Goyama et al., 2004). To produce GFP- or Cre-GFP-expressing retrovirus, we used ψMP34 packaging cells (Takara) transduced with pGCDNsam-eGFP or pGCDNsam-eGFP-iCre.

Transplantation Assays

For FL transplantation, FL cells from E14.5 wild-type or *Evi-1*$^{-/-}$ embryos (both Ly5.2) alone (noncompetitive transplants) or mixed with BM cells from wild-type mice (Ly5.1) (competitive transplants) were injected into lethally irradiated (9.5 Gy) recipient mice (Ly5.1). For BM transplantation using Cre-expressing retrovirus, c-Kit$^+$ BM progenitors from wild-type or Evi-$1^{f/f}$ mice (Ly5.2) were transduced with GFP- or Cre-GFP-expressing retroviruses and injected into sublethally irradiated (6.5 Gy) recipients (Ly5.1). For competitive transplantation using wild-type or *Evi-1*$^{+/-}$ BM cells, nucleated BM cells (Ly5.2) from each genotype were admixed in 1:1 or 1:10 ratio with competitor BM cells (Ly5.1) and injected into lethally irradiated (9.5 Gy) recipients (Ly5.1).

5FU Treatment

We used 5FU (200 mg/kg, i.p.) for myelosuppression. Peripheral blood cell counts were monitored every 5 days in each mouse.

BM Culture Assays

Lineage$^-$, c-Kit$^+$ BM progenitors were plated at a density of 10^5/ml in StemSpan serum-free medium (StemCell Technologies) supplemented with 10 μg/ml heparin, 10 ng/ml mouse SCF, 20 ng/ml mouse TPO, 20 ng/ml mouse IGF-2, and 10 ng/ml human FGF-1. Cell counts were monitored every 5 days. For the culture using Cre-expressing retroviruses, c-Kit$^+$ BM progenitors transduced with GFP or Cre-GFP were cultured in the identical condition.

Myeloid Progenitor Transformation Assays

BM progenitors (c-Kit$^+$ cells) from wild-type or Evi-$1^{f/f}$ mice were transduced with MLL/ENL or E2A/HLF oncogenes. Immortalized cells (5×10^4) from the third to fifth round of in vitro plating were subsequently transduced with either GFP- or Cre-GFP-expressing retrovirus. GFP$^+$ cells were sorted, and, then, relative clonogenic activity was assessed in the additional round of plating.

Leukemogenesis Assays In Vivo

BM progenitors (c-Kit$^+$ cells) were transduced with cMyc-bcl2 together with GFP or Cre-GFP under identical conditions to those for myeloid progenitor transformation assays. Infected progenitors (1×10^6) were injected into sublethally irradiated (6.5 Gy) recipients. For the two-step transplantation assay, BM progenitors transduced with cMyc-bcl2 were injected into recipients as described above. When transplanted mice exhibited signs of ill health, they were euthanized and their mononuclear spleen cells were isolated. Leukemic cells were then transduced with GFP- or Cre-GFP-expressing retroviruses. Secondary transplantation was performed by injecting 1×10^5 sorted GFP$^+$ cells into sublethally irradiated (6.5 Gy) recipients.

Microarray Analysis and Gene-Expression Analysis of Individuals with AML

For gene-expression profiling, total RNA was extracted from sorted cells and amplified (NuGEN Technologies, Inc.). Labeled cDNA was hybridized to the Mouse Genome 430 2.0 Array (Affymetrix). Normalization and analysis of chip data were performed using DNA-Chip Analyzer (www.dchip.org) (Li and Wong, 2001). The expression pattern of the genes in leukemic cells was assessed using gene-expression data of 285 individuals with AML (http://www.ncbi.nlm.nih.gov/geo, accession number GSE1159 [NCBI GEO]) (Valk et al., 2004). See the Supplemental Experimental Procedures for detailed analysis.

Statistical Analysis

Statistical significance of differences between parameters was assessed using a two-tailed unpaired t test. The survival distributions were compared using a log-rank test.

Cell PRESS

ACCESSION NUMBERS

All microarray data have been deposited in NCBI's Gene Expression Omnibus (GEO, http://www.ncbi.nlm.nih.gov/geo/) and are accessible through GEO Series accession number GSE11557.

SUPPLEMENTAL DATA

Supplemental Data for this article include 20 figures, 2 tables, and Supplemental Experimental Procedures and can be found with this article online at http://www.cellstemcell.com/cgi/content/full/3/2/207/DC1/.

ACKNOWLEDGMENTS

We thank T. Kitamura for Plat-E packaging cells and pMXs retroviral vector; H. Nakauchi and M. Onodera for pGCDNsam-eGFP retroviral vector; T. Nakano for OP9 stromal cells; R. Ono and T. Nosaka for MLL/ENL cDNA; T. Inaba for E2A/HLF cDNA; R. Sprengel for iCre cDNA; M.H. Tomasson for cMyc-bcl2 cDNA; N. Watanabe, Y. Kato, and A. Iwama for technical advice; R. Takizawa for help with the generation of Evi-1 mutant mice; Y. Shimamura and Y. Sawamoto for expert technical assistance; and Kirin Brewery Pharmaceutical Research Laboratory for cytokines. This work was supported in part by a Grant-in-Aid for Scientific Research from the Japan Society for the Promotion of Science and by Health and Labour Sciences Research grants from the Ministry of Health, Labour and Welfare.

Received: August 30, 2007
Revised: January 5, 2008
Accepted: June 5, 2008
Published: August 6, 2008

REFERENCES

Ayton, P.M., and Cleary, M.L. (2003). Transformation of myeloid progenitors by MLL oncoproteins is dependent on Hoxa7 and Hoxa9. Genes Dev. *17*, 2298–2307.

Barjesteh van Waalwijk van Doorn-Khosrovani, S., Erpelinck, C., van Putten, W.L., Valk, P.J., van der Poel-van de Luytgaarde, S., Hack, R., Slater, R., Smit, E.M., Beverloo, H.B., Verhoef, G., et al. (2003). High EVI1 expression predicts poor survival in acute myeloid leukemia: a study of 319 de novo AML patients. Blood *101*, 837–845.

Bonnet, D., and Dick, J.E. (1997). Human acute myeloid leukemia is organized as a hierarchy that originates from a primitive hematopoietic cell. Nat. Med. *3*, 730–737.

Bordereaux, D., Fichelson, S., Tambourin, P., and Gisselbrecht, S. (1990). Alternative splicing of the Evi-1 zinc finger gene generates mRNAs which differ by the number of zinc finger motifs. Oncogene *5*, 925–927.

Buonamici, S., Li, D., Chi, Y., Zhao, R., Wang, X., Brace, L., Ni, H., Saunthararajah, Y., and Nucifora, G. (2004). EVI1 induces myelodysplastic syndrome in mice. J. Clin. Invest. *114*, 713–719.

Calmels, B., Ferguson, C., Laukkanen, M.O., Adler, R., Faulhaber, M., Kim, H.J., Sellers, S., Hematti, P., Schmidt, M., von Kalle, C., et al. (2005). Recurrent retroviral vector integration at the Mds1/Evi1 locus in nonhuman primate hematopoietic cells. Blood *106*, 2530–2533.

Delwel, R., Funabiki, T., Kreider, B.L., Morishita, K., and Ihle, J.N. (1993). Four of the seven zinc fingers of the Evi-1 myeloid-transforming gene are required for sequence-specific binding to GA(C/T)AAGA(T/C)AAGATAA. Mol. Cell. Biol. *13*, 4291–4300.

Fears, S., Mathieu, C., Zeleznik-Le, N., Huang, S., Rowley, J.D., and Nucifora, G. (1996). Intergenic splicing of MDS1 and EVI1 occurs in normal tissues as well as in myeloid leukemia and produces a new member of the PR domain family. Proc. Natl. Acad. Sci. USA *93*, 1642–1647.

Goyama, S., Yamaguchi, Y., Imai, Y., Kawazu, M., Nakagawa, M., Asai, T., Kumano, K., Mitani, K., Ogawa, S., Chiba, S., et al. (2004). The transcriptionally active form of AML1 is required for hematopoietic rescue of the AML1-deficient embryonic para-aortic splanchnopleural (P-Sp) region. Blood *104*, 3558–3564.

Hirai, H. (1999). The transcription factor Evi-1. Int. J. Biochem. Cell Biol. *31*, 1367–1371.

Hoyt, P.R., Bartholomew, C., Davis, A.J., Yutzey, K., Gamer, L.W., Potter, S.S., Ihle, J.N., and Mucenski, M.L. (1997). The Evi1 proto-oncogene is required at midgestation for neural, heart, and paraxial mesenchyme development. Mech. Dev. *65*, 55–70.

Huntly, B.J., and Gilliland, D.G. (2005). Leukaemia stem cells and the evolution of cancer-stem-cell research. Nat. Rev. Cancer *5*, 311–321.

Izutsu, K., Kurokawa, M., Imai, Y., Maki, K., Mitani, K., and Hirai, H. (2001). The corepressor CtBP interacts with Evi-1 to repress transforming growth factor beta signaling. Blood *97*, 2815–2822.

Jin, G., Yamazaki, Y., Takuwa, M., Takahara, T., Kaneko, K., Kuwata, T., Miyata, S., and Nakamura, T. (2007). Trib1 and Evi1 cooperate with Hoxa and Meis1 in myeloid leukemogenesis. Blood *109*, 3998–4005.

Kitamura, T., Koshino, Y., Shibata, F., Oki, T., Nakajima, H., Nosaka, T., and Kumagai, H. (2003). Retrovirus-mediated gene transfer and expression cloning: powerful tools in functional genomics. Exp. Hematol. *31*, 1007–1014.

Kurokawa, M., Mitani, K., Irie, K., Matsuyama, T., Takahashi, T., Chiba, S., Yazaki, Y., Matsumoto, K., and Hirai, H. (1998). The oncoprotein Evi-1 represses TGF-beta signalling by inhibiting Smad3. Nature *394*, 92–96.

Kurokawa, M., Mitani, K., Yamagata, T., Takahashi, T., Izutsu, K., Ogawa, S., Moriguchi, T., Nishida, E., Yazaki, Y., and Hirai, H. (2000). The evi-1 oncoprotein inhibits c-Jun N-terminal kinase and prevents stress-induced cell death. EMBO J. *19*, 2958–2968.

Kustikova, O., Fehse, B., Modlich, U., Yang, M., Dullmann, J., Kamino, K., von Neuhoff, N., Schlegelberger, B., Li, Z., and Baum, C. (2005). Clonal dominance of hematopoietic stem cells triggered by retroviral gene marking. Science *308*, 1171–1174.

Lessard, J., and Sauvageau, G. (2003). Bmi-1 determines the proliferative capacity of normal and leukaemic stem cells. Nature *423*, 255–260.

Li, C., and Wong, W.H. (2001). Model-based analysis of oligonucleotide arrays: expression index computation and outlier detection. Proc. Natl. Acad. Sci. U.S.A. *98*, 31–36.

Li, Z., Chen, M.J., Stacy, T., and Speck, N.A. (2006). Runx1 function in hematopoiesis is required in cells that express Tek. Blood *107*, 106–110.

Luo, H., Li, Q., O'Neal, J., Kreisel, F., Le Beau, M.M., and Tomasson, M.H. (2005). c-Myc rapidly induces acute myeloid leukemia in mice without evidence of lymphoma-associated antiapoptotic mutations. Blood *106*, 2452–2461.

Morishita, K., Parganas, E., Parham, D.M., Matsugi, T., and Ihle, J.N. (1990). The Evi-1 zinc finger myeloid transforming gene is normally expressed in the kidney and in developing oocytes. Oncogene *5*, 1419–1423.

Morishita, K., Parganas, E., Matsugi, T., and Ihle, J.N. (1992). Expression of the Evi-1 zinc finger gene in 32Dc13 myeloid cells blocks granulocytic differentiation in response to granulocyte colony-stimulating factor. Mol. Cell. Biol. *12*, 183–189.

Mucenski, M.L., Taylor, B.A., Ihle, J.N., Hartley, J.W., Morse, H.C., 3rd, Jenkins, N.A., and Copeland, N.G. (1988). Identification of a common ecotropic viral integration site, Evi-1, in the DNA of AKXD murine myeloid tumors. Mol. Cell. Biol. *8*, 301–308.

Nitta, E., Izutsu, K., Yamaguchi, Y., Imai, Y., Ogawa, S., Chiba, S., Kurokawa, M., and Hirai, H. (2005). Oligomerization of Evi-1 regulated by the PR domain contributes to recruitment of corepressor CtBP. Oncogene *24*, 6165–6173.

Ogawa, S., Mitani, K., Kurokawa, M., Matsuo, Y., Minowada, J., Inazawa, J., Kamada, N., Tsubota, T., Yazaki, Y., and Hirai, H. (1996). Abnormal expression of Evi-1 gene in human leukemias. Hum. Cell *9*, 323–332.

Ott, M.G., Schmidt, M., Schwarzwaelder, K., Stein, S., Siler, U., Koehl, U., Glimm, H., Kuhlcke, K., Schilz, A., Kunkel, H., et al. (2006). Correction of X-linked chronic granulomatous disease by gene therapy, augmented by insertional activation of MDS1-EVI1, PRDM16 or SETBP1. Nat. Med. *12*, 401–409.

Perkins, A.S., Fishel, R., Jenkins, N.A., and Copeland, N.G. (1991). Evi-1, a murine zinc finger proto-oncogene, encodes a sequence-specific DNA-binding protein. Mol. Cell. Biol. *11*, 2665–2674.

Pintado, T., Ferro, M.T., San Roman, C., Mayayo, M., and Larana, J.G. (1985). Clinical correlations of the 3q21;q26 cytogenetic anomaly. A leukemic or myelodysplastic syndrome with preserved or increased platelet production and lack of response to cytotoxic drug therapy. Cancer *55*, 535–541.

Smith, K.S., Rhee, J.W., and Cleary, M.L. (2002). Transformation of bone marrow B-cell progenitors by E2a-Hlf requires coexpression of Bcl-2. Mol. Cell. Biol. *22*, 7678–7687.

Sood, R., Talwar-Trikha, A., Chakrabarti, S.R., and Nucifora, G. (1999). MDS1/EVI1 enhances TGF-beta1 signaling and strengthens its growth-inhibitory effect but the leukemia-associated fusion protein AML1/MDS1/EVI1, product of the t(3;21), abrogates growth-inhibition in response to TGF-beta1. Leukemia *13*, 348–357.

Sugita, M., Tanaka, N., Davidson, S., Sekiya, S., Varella-Garcia, M., West, J., Drabkin, H.A., and Gemmill, R.M. (2000). Molecular definition of a small amplification domain within 3q26 in tumors of cervix, ovary, and lung. Cancer Genet. Cytogenet. *117*, 9–18.

Suzukawa, K., Parganas, E., Gajjar, A., Abe, T., Takahashi, S., Tani, K., Asano, S., Asou, H., Kamada, N., Yokota, J., et al. (1994). Identification of a breakpoint cluster region 3′ of the ribophorin I gene at 3q21 associated with the transcriptional activation of the EVI1 gene in acute myelogenous leukemias with inv(3)(q21q26). Blood *84*, 2681–2688.

Tanaka, T., Nishida, J., Mitani, K., Ogawa, S., Yazaki, Y., and Hirai, H. (1994). Evi-1 raises AP-1 activity and stimulates c-fos promoter transactivation with dependence on the second zinc finger domain. J. Biol. Chem. *269*, 24020–24026.

Valk, P.J., Verhaak, R.G., Beijen, M.A., Erpelinck, C.A., Barjesteh van Waalwijk van Doorn-Khosrovani, S., Boer, J.M., Beverloo, H.B., Moorhouse, M.J., van der Spek, P.J., Lowenberg, B., et al. (2004). Prognostically useful gene-expression profiles in acute myeloid leukemia. N. Engl. J. Med. *350*, 1617–1628.

Yuasa, H., Oike, Y., Iwama, A., Nishikata, I., Sugiyama, D., Perkins, A., Mucenski, M.L., Suda, T., and Morishita, K. (2005). Oncogenic transcription factor Evi1 regulates hematopoietic stem cell proliferation through GATA-2 expression. EMBO J. *24*, 1976–1987.

Zhang, C.C., and Lodish, H.F. (2005). Murine hematopoietic stem cells change their surface phenotype during ex vivo expansion. Blood *105*, 4314–4320.

AML1/Runx1 Negatively Regulates Quiescent Hematopoietic Stem Cells in Adult Hematopoiesis[1]

Motoshi Ichikawa, Susumu Goyama, Takashi Asai, Masahito Kawazu, Masahiro Nakagawa, Masataka Takeshita, Shigeru Chiba, Seishi Ogawa, and Mineo Kurokawa[2]

Transcription factor AML1/Runx1, initially isolated from the t(8;21) chromosomal translocation in human leukemia, is essential for the development of multilineage hematopoiesis in mouse embryos. AML1 negatively regulates the number of immature hematopoietic cells in adult hematopoiesis, whereas it is required for megakaryocytic maturation and lymphocytic development. However, it remains yet to be determined how AML1 contributes to homeostasis of hematopoietic stem cells (HSCs). To address this issue, we analyzed in detail HSC function in the absence of AML1. Notably, cells in the Hoechst 33342 side population fraction are increased in number in AML1-deficient bone marrow, which suggests enrichment of quiescent HSCs. We also found an increase in HSC number within the AML1-deficient bone marrow using limiting dilution bone marrow transplantation assays. These results indicate that the number of quiescent HSCs is negatively regulated by AML1. ***The Journal of Immunology,*** **2008, 180: 4402–4408.**

Mammalian hematopoietic development is believed to derive from two distinct cellular origins. In mice, generation of the primitive erythroid lineage consisting of large and nucleated erythrocytes, known as primitive hematopoiesis, occurs around day 7.5 postcoitus in the yolk sac (1). The second wave of hematopoiesis, which is called definitive hematopoiesis and consists of enucleated erythrocytes, myeloid cells, and lymphoid progenitors, emerges later in the fetal liver around day 9.5 postcoitus and results in expansion of hematopoietic stem cells (HSCs)[3] and generation of blood cells (2, 3). At the center of stem cell self-renewal and lineage commitment decisions lie the precisely regulated expression levels of lineage-specific transcription factors. The role of specific transcription factors in hematopoietic stem cell fate decisions has derived largely from genetic strategies, primarily gene-targeting and transgenic or retroviral overexpression experiments. From the growing body of experimental results, several transcription factors have been found to play critical roles in hematopoietic stem cell physiology.

Transcription factor AML1, also known as RUNX1, CBFA2, or PEBP2αB, is initially isolated from the breakpoint of t(8;21) chromosomal translocations found in acute myelogenous leukemia (AML) (4) and is recognized as one of the most important transcription factors which regulate mammalian hematopoietic homeostasis. AML1 is specifically required for the development of definitive hematopoiesis in the embryonic stage as shown by gene-targeting experiments in mice (5, 6). In contrast, as we and others have previously shown, loss of AML1 in the adult stage does not cause complete loss of hematopoiesis (7–9). AML1-deleted adult mice show a decrease in platelets due to a maturational defect of the megakaryocytes as well as block of lymphocyte development, while the fraction of immature hematopoietic progenitors is expanded (7). These results suggest that AML1 is not required for the maintenance of HSCs, but for the differentiation and maturation of more committed cells. It is also suggested that embryonic development of hematopoiesis and maintenance of adult hematopoiesis is, respectively, regulated by distinct molecular mechanisms, which is also supported by analyses on conditional knockout mice which target hematopoietic genes, such as *SCL* and *NOTCH1* (10, 11).

Impaired function of AML1 in the hematopoietic system is associated with a variety of human hematological malignancies including t(8;21)-positive AML, immature-type AML defined as M0 by French-American-British classification (12), myelodysplastic syndromes (13), and familial platelet disorder with propensity to AML (14). Mice with bone marrow cells that express leukemic chimeric protein AML1/ETO (AML1/MTG8) produced by t(8;21) chromosomal translocation do exhibit a myeloproliferative phenotype, which was susceptible to the development of leukemia when the mice were treated with alkylating agents to induce additional genetic aberrations (15–19). Because AML1/ETO acts dominant-negatively over normal AML1 function, the myeloproliferative phenotype has been explained by the expansion of the HSC fraction in these mice caused by suppressed AML1 activities. As is recently reported, however, introduction of a splicing variant form of AML1/ETO in the bone marrow cells causes the development of leukemia in mice independently of second-hit mutations by alkylating agents (20). In addition, AML1-deficient bone marrow cells fail to show infinite replating capacity in contrast to AML1/ETO-expressing bone marrow cells (7). Therefore, the expansion of hematopoietic stem cells of AML1/ETO may not be caused only

Department of Hematology and Oncology, Graduate School of Medicine, University of Tokyo, Tokyo, Japan

Received for publication May 3, 2007. Accepted for publication January 21, 2008.

The costs of publication of this article were defrayed in part by the payment of page charges. This article must therefore be hereby marked *advertisement* in accordance with 18 U.S.C. Section 1734 solely to indicate this fact.

[1] This work was supported in part by grants from the Ministry of Education, Culture, Sports, Science and Technology (KAKENHI 18013014 to M.K.), Japan Society for the Promotion of Science (Grant-in-Aid for Fellows 17-10666 to M.I.), and the Ministry of Health, Labour and Welfare (Health and Labour Sciences Research Grants to M.K.).

[2] Address correspondence and reprint requests to Dr. Mineo Kurokawa, Department of Hematology and Oncology, Graduate School of Medicine, University of Tokyo, Bunkyo-ku, Tokyo, 113-8655, Japan. E-mail address: kurokawa-tky@umin.ac.jp

[3] Abbreviations used in this paper: HSC, hematopoietic stem cell; 7-AAD, 7-aminoactinomycin D; SP, side population; KSL, lineage-negative, c-Kit-positive, and Sca-1-positive; cKO, conditional knockout; CRU, competitive repopulating unit; Ct, cycle threshold; GMP, granulocyte-macrophage progenitor; CMP, common myeloid progenitor.

by suppression of AML1 function, but other molecular pathways used by the ETO portion are necessary for the development of leukemia. In contrast to our observation that AML1- deficient bone marrow contains expanded hematopoietic progenitors, it has been reported that bone marrow cells with the heterozygously inactivated *AML1* locus show a decrease in competitive repopulating capacity (21) and lower chimerism in long-term competitive repopulation assays (9). Therefore, it is essential to know whether deletion of AML1 causes expansion of the most primitive hematopoietic stem cells to understand the molecular mechanisms of hematological malignancies related to abnormal AML1 functions. To address this issue, we analyzed in detail HSC function in the absence of AML1 using conditional AML1 knockout mice.

Materials and Methods

Animals

AML1 conditional knockout mice (7) were crossed with *Mx-cre* transgenic mice (22) and maintained at the C57BL/6J background at the Section of Animal Research, Division of Research Resources and Support, Center for Disease Biology and Integrative Medicine, Faculty of Medicine (University of Tokyo, Tokyo, Japan). C57BL/6J mice were purchased from Clea Japan. Mice congenic for the Ly5 locus (C57BL/6-Ly5.1), bred and maintained at Sankyo Labo Service (Tsukuba, Japan), were provided by Dr. H. Nakauchi (Institute of Medical Science, University of Tokyo, Tokyo, Japan).

The genotypes of the wild-type *AML1* (*AML1*^{wt}), *lox*P-flanked (*AML1*^{fl}), and deleted (*AML1*$^{-}$) loci were analyzed using genomic PCR primers as described previously (7). To induce excision of *AML1* in the adult mice, *AML1*$^{fl/fl}$ *Mx-cre*-transgenic mice were i.p. injected with poly(I:C) (Sigma-Aldrich) along with littermate control mice at the age of 5–10 wk, and bone marrow cells were collected 4–9 wk after poly(I:C) injection. The age of mice was between 12 and 19 wk at the time of bone marrow collection. In limiting dilution bone marrow transplantation assays, 500 μg of poly(I:C) was injected seven times on alternate days to maximize the gene deletion. Because a high dose of poly(I:C) caused exhaustion of some mice, 250 μg of poly(I:C) was administered three times (days 1, 3, and 5) in other experiments, since this administering schedule caused effective deletion of the *AML1* locus (7).

All animal studies were approved by the institutional review board, following institutional guidelines for animal researches.

Bone marrow transplantation

Bone marrow cells were collected by flushing the femurs and tibiae of the mice with 22-gauge needles into 5 ml of RPMI 1640 medium supplemented with 2% FBS and nucleated cells were counted. For transplantation, nucleated cells were counted as indicated and i.v. injected into lethally irradiated (9 Gy) female, 8- to 10-wk-old C57BL/6J mice. The x-ray irradiation was performed using MBR-1505R2 apparatus (Hitachi Medical). For transplantation of retrovirus-transduced hematopoietic cells, C57BL/6-Ly5.1 mice were i.p. injected with 150 mg/kg 5-fluorouracil (Sigma-Aldrich). Five days after injection, mononuclear cells from two to four mice were precultured in a cytokine-containing medium for retrovirus infection overnight and transduced with retrovirus medium for 3 days. Transduced cells were purified with FACSAria flow cytometer using "yield" mode at a purity of 70–90%, and 3–4 $\times$ 10^5 purified cells were coinjected with 1 $\times$ 10^5 normal C57BL/6J bone marrow cells to irradiated (9 Gy) C57BL/6J recipient mice.

Real-time PCR for chimerism assays

Bone marrow cells from one femur and two tibiae were collected into 1 ml of RPMI 1640 medium supplemented with 2% FBS, and the genomic DNA was purified from 100 μl of cell suspension using an MFX-9600 apparatus and a NPK-391 magnetic bead-based genomic DNA extraction kit (Toyobo) according to the manufacturer's instructions. Chimerism assays using real-time PCR were done as previously described (23). Briefly, male bone marrow cells were serially diluted with female bone marrow cells (to contain 0, 0.1, 0.3, 1, 3, 10, 30, and 100% of male cells) for establishing standard curves, and the genomic DNA was subjected for real-time PCR amplification for *Zfy2* (primers 5′-TGG AGA GCC ACA AGC TAA CCA-3′ and 5′-TCC CAG CAT GAG AAA GAT TCT TC-3′) and *GAPDH* (primers 5′-GGA GAT TGT TGC CAT CAA CG-3′ and 5′-GTC TCG CTC CTG GAA GAT GG-3′) using the SYBR Green PCR reagent kit (Invitrogen Life Technologies) and Applied Biosystems 7000 Sequence Detector. For each sample and standard mixture, cycle threshold readings (Ct) were determined using the Sequence Detection Software (Applied Biosystems) and the ΔCt (= (Ct for *Zfy2*) − (Ct for *GAPDH*) amplified from each of the same sample) value was calculated. A standard curve was generated by plotting the known percentage of male DNA to the logarithmic y-axis and ΔCt values to the linear *x*-axis. The detection limit of male cells in this assay was estimated to be ~0.3%. Excision of the Aml1 locus was confirmed for the samples with high male chimerism using nested PCR as described previously (7).

Flow cytometry

Staining bone marrow cells for Hoechst 33342 side population (SP) cell fraction and G_0 cell cycle fraction was done as described previously (24–26). Flow cytometry was performed using BD LSR II apparatus (BD Biosciences) for nonsorting analyses and FACSAria apparatus (BD Biosciences) for sorting experiments. The following mAbs were used for analyses on hematopoietic stem cells: FITC-conjugated rat mAb to CD34 (clone RAM34; BD Biosciences), PE-conjugated Ab to Sca-1 (clone D7; BD Biosciences), biotin-conjugated Ab to CD3ε, CD4, CD8a, B220, Gr-1, Mac-1, and TER-119 (clones 145-2C11, RM4-5, 53-6.7, RA3-6B2, RB6-8C5, M1/70, and TER-119; all from BD Biosciences, except for CD8a and Gr-1 Abs from eBioscience) visualized by PerCP-conjugated streptavidin; BD Biosciences) and allophycocyanin-conjugated Ab to c-Kit (clone 2B8; BD Biosciences). For the analysis of the G_0 cell cycle status of the cells in the KSL fraction, cells were first stained with FITC-conjugated Ab to lineage Ags listed above (all from BD Biosciences, except for TER-119 Ab from Medical & Biological Laboratories) and negative fraction was collected using MACS anti-FITC Ab and an AutoMACS apparatus (Miltenyi Biotec) according to the manufacturer's instructions. c-Kit-positive cells were then collected using a MACS anti-c-Kit Ab and AutoMACS (Miltenyi Biotec) and stained for allophycocyanin-conjugated Ab to Sca-1 (clone D7; eBioscience) and pyronin-Y. Cell cycle status was assayed for cells in the FITC-negative, allophycocyanin-positive gates. For other sorting analyses, cells were stained using FITC-conjugated Ab to CD34, PE-conjugated Ab to CD16/32 (FcγRIII/II; clone 2.4G2; eBioscience), biotin-conjugated lineage Ag listed above followed by visualization with SA-PerCP, PE-Cy7-conjugated Ab to Sca-1 (clone E13-161.7; eBioscience), and allophycocyanin-conjugated Ab to c-Kit. For analyzing lineage-negative (Lin$^-$) cells, dead cells were excluded from analyses along with lineage-positive cells by staining the cells with 7-aminoactinomycin D (7-AAD, Via-Probe; BD Biosciences). Acquired data were analyzed using FACSDiva or CellQuest software (BD Biosciences).

Colony assays

Determined numbers of cells were collected in IMDM supplemented with 2% FBS and cultured in MethoCult GF M3434 methylcellulose-based medium (Stem Cell Technologies) per the manufacturer's instructions. Cell clusters consisting of 50 cells or more were counted as colonies and colonies were differentially scored according to their morphology at day 7 of culture.

Retrovirus infection

Mouse *AML1* cDNA was subcloned into pGCDNsam-IRES-GFP (a gift from Dr. H. Nakauchi, Institute of Medical Science, University of Tokyo, Tokyo, Japan), and viral supernatants from the empty vector (mock) and *AML1* vector were produced using the MP34 packaging cell line as previously described (27). Transduction was performed using Retronectin (Takara Bio) according to the manufacturer's instructions in RPMI 1640 supplemented with 10% FBS, 10 ng/ml mouse stem cell factor, 6 ng/ml mouse IL-3, and 10 ng/ml mouse IL-6 (cytokines provided by Kirin Brewery) at a cell density of ~10,000–40,000 cells/well on 24-well nontreated culture plates (Nunc) for purified hematopoietic progenitor cells or 4–8 $\times$ 10^5 cells/well on 6-well nontreated culture plates (Nunc) for nonsorted mononuclear cells. Three days after culture in the retrovirus-containing medium, cells were sorted using FACSAria for GFP positivity.

Statistical analyses

Competitive repopulating units (CRUs) were calculated using the StatMod package for the GNU R statistical analysis software. Flow cytometry data from mouse littermate pairs were first examined using the *F* test for equality of variance and then compared using the paired or unpaired *t* test if applicable. When equality of variance was rejected, paired data were tested by Wilcoxon's signed rank test.

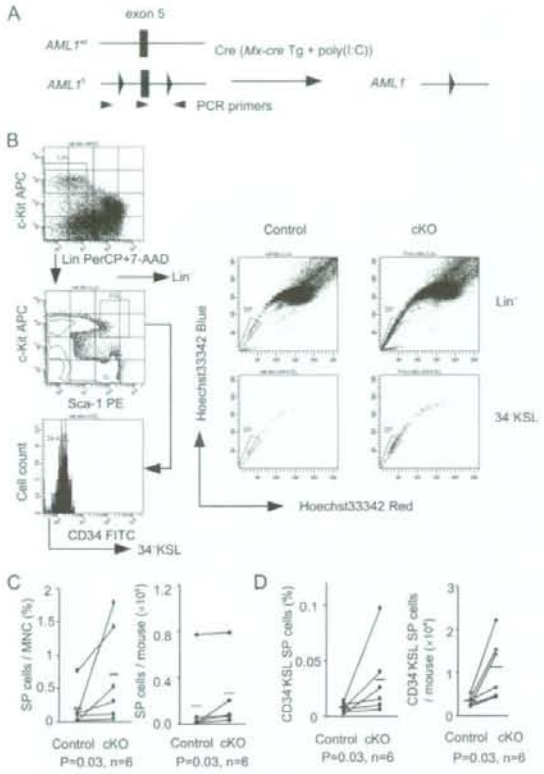

FIGURE 1. Hoechst 33342 SP analysis of the bone marrow cells from conditional AML1 knockout (cKO) mice. *A*, Schematic representation of the cKO alleles. *B*, SP cell profiles of Lin^- and $CD34^-$ KSL populations from cKO and control mice. *C* and *D*, Statistical analyses of the SP fraction from cKO and control bone marrow cells. Percentage of cells in the SP fraction (shown in *B*) from each paired (cKO and control littermates) experiments are displayed as paired data. *C*, Numbers of the Lin^- SP cells (frequencies within mononuclear gates and absolute numbers per mouse). *D*, SP fraction cells within $CD34^-$ KSL cells as frequencies within mononuclear gates and absolute numbers per mouse. Mean SP percentages are shown as bars in these graphs. Because equality of the variance of the data were rejected by the *F* test, *p* values were calculated using Wilcoxon's signed rank test. Tg, Transgenic.

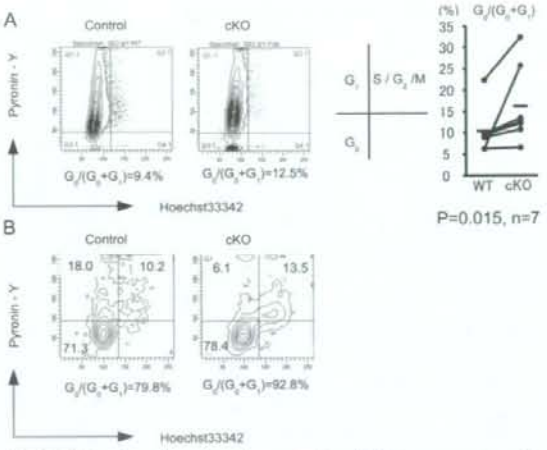

FIGURE 2. G_0 cell cycle analyses on the c-Kit^+ bone marrow cells from cKO mice. *A*, Bone marrow cells from cKO and control mice that are c-Kit^+ are assayed for G_0 cell fractions. G_0 and G_1 cells were gated according to Hoechst 33342 fluorescence. G_0 cells were defined as cells the p-Y fluorescence of which is below those of G_2-M cells (Hoechst-high cells). The value of *p* was calculated using Wilcoxon's signed rank test. *B*, Similar assays were performed on bone marrow cells sorted by Lin^- c-Kit^+ cells and stained with allophycocyanin-conjugated Ab to Sca-1. Representative data within Sca-1^+ gates from two independent experiments.

Results

Number of quiescent hematopoietic stem cells in the bone marrow is negatively regulated by AML1

We previously reported the increased cell number of the $CD34^-$, Lin^-, c-Kit^+, and Sca-1^+ ($CD34^-$ KSL) fraction, in which long-term hematopoietic stem cells are concentrated in the bone marrow of the conditional knockout mice that delete AML1 after birth (7). AML1-deficient cells contribute to the granulocytic lineage of the recipient mice more efficiently than control cells at 1 mo after transplantation, when both of them are transplanted into lethally irradiated mice in the competitive repopulation experiments. However, the contribution of the AML1-deficient cells to granulocytes in the peripheral blood tends to decrease over time (7). Therefore, we sought to determine precisely whether HSCs are increased in the bone marrow of AML1-deficient mice. We crossed conditional AML1 knockout mice with *lox*P-flanked exon 5 in the *AML1* locus (*AML1*^{fl}, Fig. 1*A*) (7) with IFN-inducible *Mx-cre*-transgenic mice (22) to generate *AML1*$^{fl/fl}$ *Mx-cre* mice, in which we can induce *AML1* excision at the adult stage by injecting poly(I:C). Although deletion of the *lox*P-flanked *AML1* loci in the bone marrow cells was almost complete after three injections of poly(I:C) at a dose of 250 μg, we used a higher dose (seven injections of 500 μg of poly(I:C)) in transplantation experiments to maximize the gene deletion, because a trace number of HSCs may expand and affect the data. *AML1*$^{wt/wt}$ *Mx-cre* mice or *AML1*$^{fl/fl}$ mice without the *Mx-cre* transgene were treated with poly(I:C) and used as controls. HSCs that can reconstitute adult hematopoiesis for a long term are concentrated in the Hoechst 33342 SP fraction, which represents quiescent stem cells with the ability to efflux the dye at a greater rate than the other major part of the cells (main population) (24). Although the total number of cells in the AML1-deficient bone marrow was not significantly different from that of conditional knockout (cKO: $4.73 \pm 2.11 \times 10^7$ vs control: $5.74 \pm 2.86 \times 10^7$, $p = 0.50$), the SP cell fraction within the bone marrow cells and the absolute number of SP cells per mouse was significantly increased in AML1-deficient mice compared with control mice, suggesting that quiescent HSCs are increased in the absence of AML1 (Fig. 1, *B* and *C*). Among SP cells, quiescent HSCs are known to be further concentrated in the fraction that has the $CD34^-$ KSL surface marker phenotype ($CD34^-$ KSL SP cells) (26). $CD34^-$ KSL SP cells were also increased in the AML1-deficient mice (Fig. 1, *B* and *D*), again indicating the increase in the quiescent HSC number in the AML1-deficient bone marrow. Given the elevated number of SP cells in the absence of AML1, we next analyzed the cell cycle status of immature hematopoietic cells to determine the number of cells within the G_0 state. We stained the bone marrow cells with a stem cell-related surface marker c-Kit, DNA dye Hoechst 33342 and RNA dye pyronin-Y. As shown in Fig. 2*A*, the G_0 fraction defined as cells that show 2n DNA content by Hoechst 33342 staining and low RNA by pyronin-Y staining is also increased in the c-Kit^+ bone marrow cells of AML1-deficient mice. We then sorted KSL cells, in which HSCs are concentrated, and found an increase of the G_0 KSL cells in the AML1-deficient

Table I. *Quantification of CRUs of the bone marrow*[a]

Injected Cell No.	$AML1^{fl/fl}$ *Mx-cre*	$AML1^{fl/wt}$ *Mx-cre*	$AML1^{wt/wt}$ *Mx-cre*
30,000	8/8	3/6	1/6
10,000	7/8	1/6	2/8
3,000	2/8	0/6	2/8
1,000	2/8	3/8	0/6
HSC frequency	1 in 5,606	1 in 29,531	1 in 52,043
(95% confidence interval)	(3,085–10,186)	(13,326–65,441)	(20,688–130,925)

[a] For each indicated number of transplanted cells from $AML1^{fl/fl}$ *Mx-cre*, $AML1^{fl/wt}$ *Mx-cre*, and $AML1^{wt/wt}$ *Mx-cre* male mice, the proportion of mice that are positive for test male cells is given as (number of positive mice)/(number of analyzed mice). Frequencies of HSCs were calculated using Poisson statistics. Representative data from two independent experiments are shown.

mice (Fig. 2*B*), indicating that loss of AML1 causes an increase of immature hematopoietic cells in the quiescent state.

Because the fractions in which HSCs are concentrated have increased in the AML1-deficient mice, we assessed CRUs contained in the AML1-deficient mice using a bone marrow transplantation assay with limiting dilution to determine the frequency of long-term HSCs (28). Bone marrow cells from $AML1^{fl/fl}$ *Mx-cre*, $AML1^{fl/wt}$ *Mx-cre*, or $AML1^{wt/wt}$ *Mx-cre* male mice treated with poly(I:C) were serially diluted, cotransplanted with 2×10^5 female competitor bone marrow cells into the lethally irradiated wild-type female C57BL/6J mice, and then donor cell chimerism was evaluated in the reconstituted bone marrow. Because nucleated cells in the peripheral blood are predominantly lymphocytes in mice and AML1-deficient lymphocyte progenitors show maturation block at early stages (7, 9), we used bone marrow cells rather than peripheral blood cells for the analysis for repopulation to avoid underestimation. At 4 mo after transplantation, genomic DNA was purified from the bone marrow cells. Donor cell chimerism was assayed using quantitative real-time genomic PCR targeted for the *Zfy* locus, which is specific for the Y chromosome (23). Mice with ≥1% test cell chimerism were treated as positive for donor cell engraftment, and CRUs were evaluated using proportions of engrafted mice and numbers of transplanted cells (28). As shown in Table I and Fig. 3*A*, there was ~10-fold increase in CRUs in AML1-deficient bone marrow in comparison to control mice. PCR genotyping confirmed almost complete deletion of the *AML1* locus of the $AML1^{fl/fl}$ *Mx-cre* bone marrow cells (Fig. 3*B*). CRUs in the bone marrow of mice with heterozygously deleted *AML1* locus ($AML1^{fl/wt}$ *Mx-cre* mice treated with poly(I:C)) showed a slight but not statistically significant increase in number compared with control mice. These results indicate that loss of AML1 causes expansion of long-term HSCs in the bone marrow.

Because the number of hematopoietic stem cells appeared to be inversely correlated to the attenuated doses of AML1, we next examined the effect of forced expression of AML1 on HSC activity. Bone marrow cells from $Ly5.1^+$ C57BL/6 congenic mice were transduced with retroviruses expressing GFP alone or along with AML1 (27). After the infection, GFP^+ cells were sorted and i.v. injected into lethally irradiated $Ly5.2^+$ wild-type C57BL/6J mice along with supporting cells. Four weeks after transplantation, donor cell chimerism in the bone marrow was assayed by flow

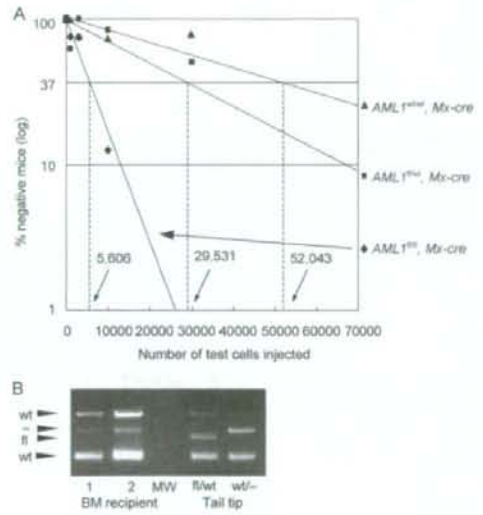

FIGURE 3. Limiting dilution analysis based on competitive repopulation. *A*, Varying numbers of bone marrow cells from male $AML1^{fl/fl}$, *Mx-cre* (♦), $AML1^{fl/wt}$, *Mx-cre* (■), or $AML1^{wt/wt}$, *Mx-cre* (▲) mice were mixed with 2×10^5 bone marrow cells from female C57BL/6J mice and injected into lethally irradiated C57BL/6J female mice. Reconstitution in the bone marrow was evaluated at 4 mo after transplantation. Mice were considered negative when the percent chimerism was <1.0. Estimated frequencies of the repopulating cells are indicated as vertical dashed lines (1 repopulating cell per indicated numbers of bone marrow cells) for each genotype. Representative data from two independent experiments are shown. *B*, Genomic PCR analysis of the bone marrow cells reconstituted by $AML1^{fl/fl}$, *Mx-cre* mice in the same experiment (*two lanes* at the *left*). Control PCR fragments using tail tip DNA from $AML1^{fl/wt}$ and $AML1^{wt/-}$ mice (*two lanes* at the *right*) are also displayed to indicate the position of the PCR products generated from each type of AML1 allele. wt, Wild type.

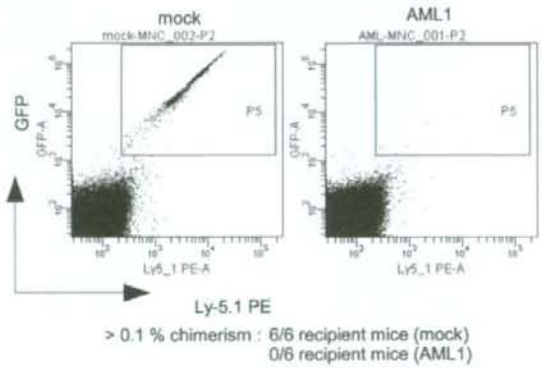

FIGURE 4. Hematopoietic reconstitution by AML1-overexpressing bone marrow cells. Bone marrow cells from C57BL/6-Ly5.1 mice were infected with mock or AML1-expressing retrovirus containing GFP, collected for expression of GFP and transplanted into C57BL/6J (Ly5.2) mice. Reconstituted bone marrow cells at 4 wk after transplantation were stained with 7-AAD viability dye and PE-conjugated Ab to Ly-5.1 (CD45.1). Representative dot plots within 7-AAD-negative cell gates are shown.